Generating Physics-based Mass Estimating Relationships:

A Test Case Using LOX-Tank Bending Loads Applied to the Forward LH_2 Tank of the Georgia Tech Air Breathing Launch Vehicle

Leland R. Marcus

AE 8900 Special Project
December 14, 2001

School of Aerospace Engineering
Georgia Institute of Technology

Advisor: Dr. John R. Olds

TABLE OF CONTENTS

LIST OF FIGURES

LIST OF TABLES

I. INTRODUCTION

This paper is written in support of the on-going research into conceptual space vehicle design conducted at the Space Systems Design Laboratory (SSDL) at the Georgia Institute of Technology. Research at the SSDL follows a sequence of a number of the traditional aerospace disciplines. The sequence of disciplines and interrelationship among them is shown in the Design Structure Matrix (DSM) shown in Figure 1.

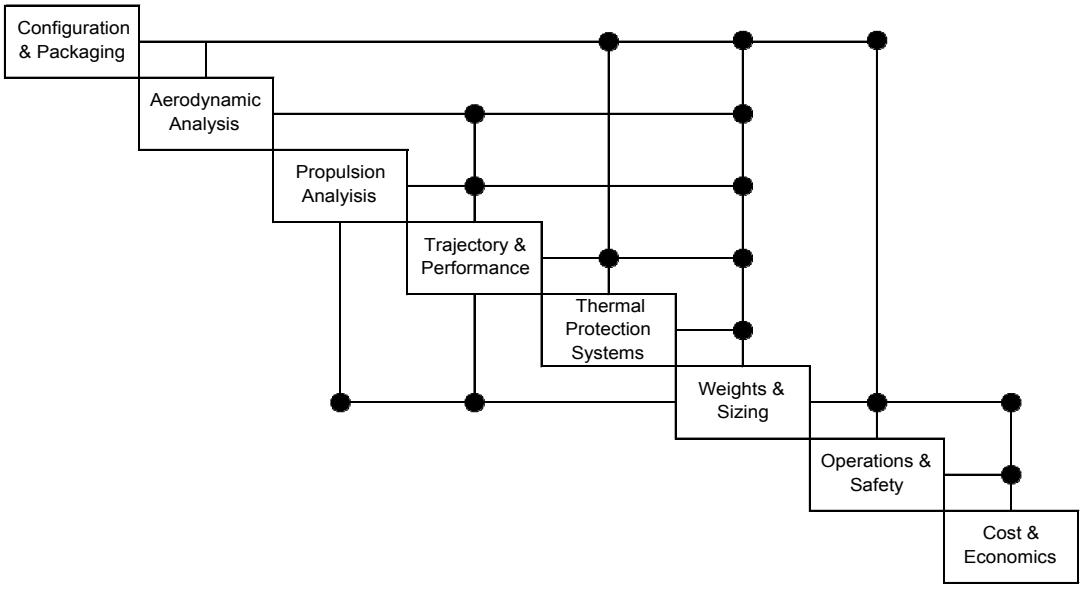

FIGURE 1: DESIGN STRUCTURE MATRIX

It is easily seen from Figure 1 that the discipline of Weights and Sizing occupies a central location in the design of a new space vehicle. Weights and Sizing interacts, either in a feed forward or feed back manner, with every other discipline in the DSM. Because of this principal location, accuracy in Weights and Sizing is integral to producing an accurate model of a space vehicle concept.

It is in the process of transferring a vehicle from conceptual design to detailed design that shows the flaws of the current method of conducting Weights and Sizing analysis in conceptual design. In conceptual design, Weight Estimating is conducted using Mass Estimating Relationships (MERs) based on historical data from previous

vehicles or designs. It isn't until detailed design begins that the physics-based analysis of finite element structural analysis is conducted. Finite Element Analysis (FEA) is a much higher fidelity analysis than MERs, but it is also a much more time consuming process and thus not suited to the fluid design space and rapid analysis of conceptual design.

Until now, the historical nature of MERs has not been a source of great difficulty because new vehicle designs use geometries and materials similar to those vehicles, primarily Expendable Launch Vehicles (ELVs), in the database used to create the MERs. The next step in Reusable Launch Vehicle (RLV) design will break this paradigm.

FIGURE 2: SATURN V and X-43

Generation 2 and beyond RLVs will be made of new, mainly composite, materials and will use vehicle geometries radically different from the past. (See Figure 2.) One proposed solution to this problem is the use of a Technology Reduction Factor (TRFs) to account for the difference in mass due to a change in material and a Geometric Factor

(GF) to account for differences in geometry [1]. However, both of these factors are extremely difficult to estimate accurately. Instead of using additional conceptual level techniques, a simplified FEA technique is described in this paper, as applied to the problem of the Liquid Oxygen (LOX) tank bending loads applied to the forward Liquid Hydrogen (LH_2) tank of the Georgia Tech Air Breathing Launch Vehicle (ABLV).

II. BACKGROUND

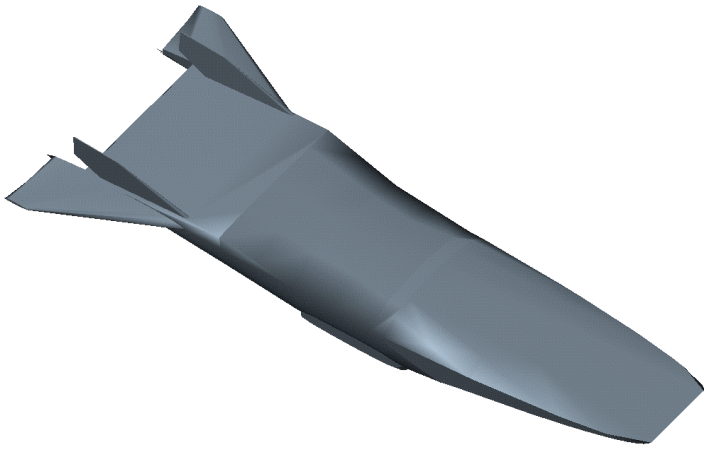

FIGURE 3: Georgia Tech ABLV Outer Mold Line

The Georgia Tech ABLV, shown in Figure 3, is a Rocket Based Combined Cycle (RBCC) RLV. The fuel tanks, shown in red in Figure 4, hold all the LH_2 required for the entire ascent trajectory. The oxidizer is taken from the atmosphere during various phases of the trajectory, before the vehicle switches to the all-rocket mode. In all-rocket mode, the oxidizer, LOX, is supplied from tanks, shown in blue in Figure 4, located amidships and close to the vehicle center of gravity.

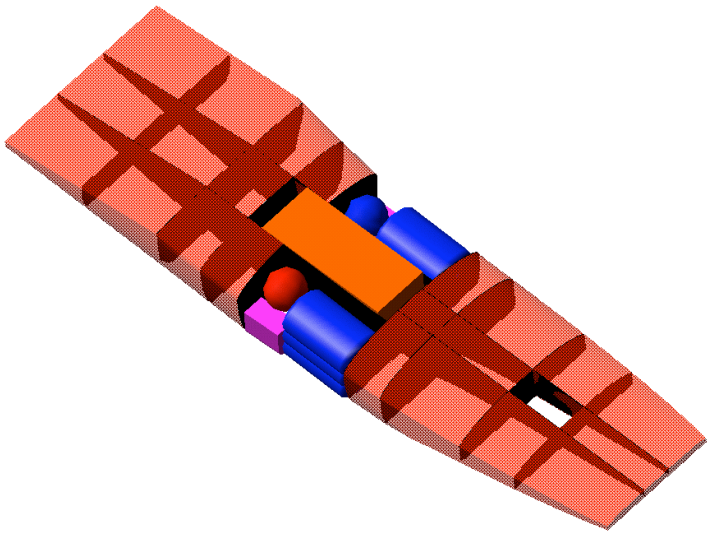

FIGURE 4: Georgia Tech ABLV Tank Configuration

A similar air breathing vehicle concept is under development at NASA's Langley Research Center (LaRC). This design places the LOX tanks forward and aft rather than amidships. This gives a greater moment of inertia about the pitch axis, in an attempt to improve flight dynamics stability. Problematically, this applies a bending load to the forward LH2 tank that is not accounted for in the previous analysis. The suggested solution for this additional load is a multiplicative factor, shown in Figure 5, applied to the unit tank mass.

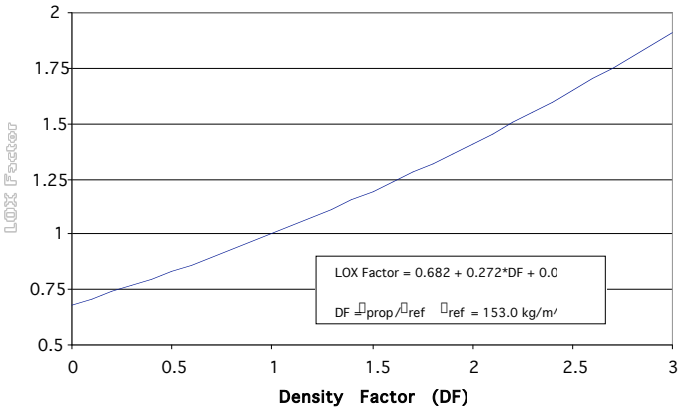

FIGURE 5: The LOX Factor

The equation given in Figure 5 is a function of Density Factor (DF), which is the ratio of ρ_{prop} to ρ_{ref}, where ρ_{ref} = 153.0 kg/m3. ρ_{prop} is assumed to be bulk density and some additional assumptions are made in the Analysis section. Based on those assumptions, this paper attempts to recreate and validate the LOX Factor.

III. METHOD OF SOLUTION

A. DESIGN OF EXPERIMENTS

The Multidisciplinary Design Optimization (MDO) technique used in this analysis is the approximate, or parameter, method of Design of Experiments (DOE). This technique takes data at strategic locations of the design space and then uses it to form the basis for generating a model of the entire space. This simulation is created by generating a Response Surface Equation (RSE) based on the DOE results. The design variables that are used in a DOE are called factors, and the values at which factors are evaluated are called levels.

Table 1: CCD Factors and Normalized Levels

Run	Length	Aero Load	Nose Load
1	-1	-1	-1
2	-1	-1	1
3	-1	1	-1
4	-1	1	1
5	1	-1	-1
6	1	-1	1
7	1	1	-1
8	1	1	1
9	0	0	0
10	-1	0	0
11	1	0	0
12	0	-2	0
13	0	2	0
14	0	0	-1
15	0	0	1

Because a generic two level DOE only allows for the construction of a linear RSE, additional runs are included to create a multi-level Central Composite DOE. By adding seven runs a quadratic model can be generated. The levels for each factor in a specific run are given in Table 1.

Tank length, aerodynamic load, and nose load are the three design variables selected as factors. Tank length is selected to give a feel for the effect of changing the tank fineness ratio on a range of approximately 1 to 2, based on a constant width of 12 meters. Aerodynamic load is selected to allow for the composite effect of a variation of vehicle gross lift-off weight and vehicle lift. The vehicle is assumed to have a gross lift-off mass of 500,000 kg, corresponding to approximately 5000 kN. This weight must be supported in flight by lift generated by flow over the body. The required lift provided by the forward tank is centered at 60% of lift off weight, and varied from 20% to 100%. Nose load is centered at 2500 kN, equivalent to approximately 100,000 kg of LOX (assuming 2.5 g's), with variation from zero (no LOX tank) up to 5000 kN. Additionally, the design variable of internal pressure is not assigned as a factor and was set to a constant value of 3 atm absolute, equivalent to 2 atm gage on the pad. Analysis was for a 2 atm load. The values for each factor and level are summarized in Table 2.

Table 2: CCD Factors and Equivalent Levels

	-□	-1	0	1	□
Length (m)	10	10	15	20	20
Aero Load (kN)	1000	2000	3000	4000	5000
Nose Load (kN)	0	0	2500	5000	5000

With the results of these runs, the RSE for Tank Mass is generated using the following form:

$$M = \square_0 + \square_1 L + \square_2 A + \square_3 N + \square_4 LA + \square_5 LN + \square_6 AN + \square_7 L^2 + \square_8 A^2 + \square_9 N^2$$

Where M is tank mass in kg, L is tank length in m, A is aerodynamic load in kN, and N is tank nose load in kN. The coefficients are found from regression against the 15 results of the DOE.

B. PATRAN/NASTRAN FEA

FEA is conducted using the NASTRAN FEA code and the PATRAN geometry pre- and post-processor code. PATRAN is used to create the various geometric models, associate elements to the geometry, and then assign materials, loads and boundary conditions to the elements. Then NASTRAN is used to analyze the model for displacements and stresses. The NASTRAN output is then returned to PATRAN to generate stress contour plots superimposed on the geometry. Simultaneously, the NASTRAN output is sent to an Excel workbook to reduce and analyze the data before a second Excel workbook regresses the final MER. A flowchart of this process is given in Figure 6.

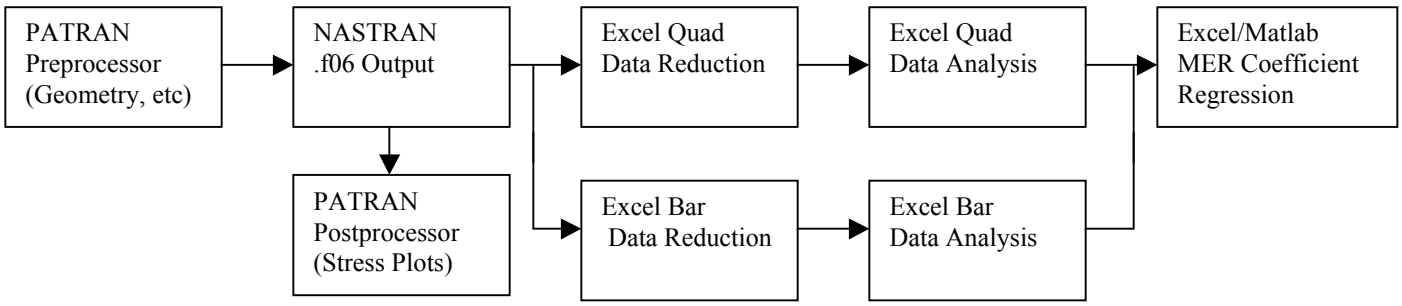

FIGURE 6: Process Flow

1. Geometry

Three different geometries are generated, one each for a vehicle length of 10 meters, 15 meters, and 20 meters. All three models have the same sized front panel, 1

meter by 12 meters, and back panel, 5 meters by 12 meters. The top of each panel is at the same height. Then the distance between these two panels is varied to change the length of the tank. Reinforcement grids composed of a mesh of bar elements (but with no panel elements) are placed at five-meter increments inside the tanks. Thus, the 10-meter tank has only one grid while the 20-meter tank has three. Wireframe versions of the tanks are shown in Figures 7 to 9.

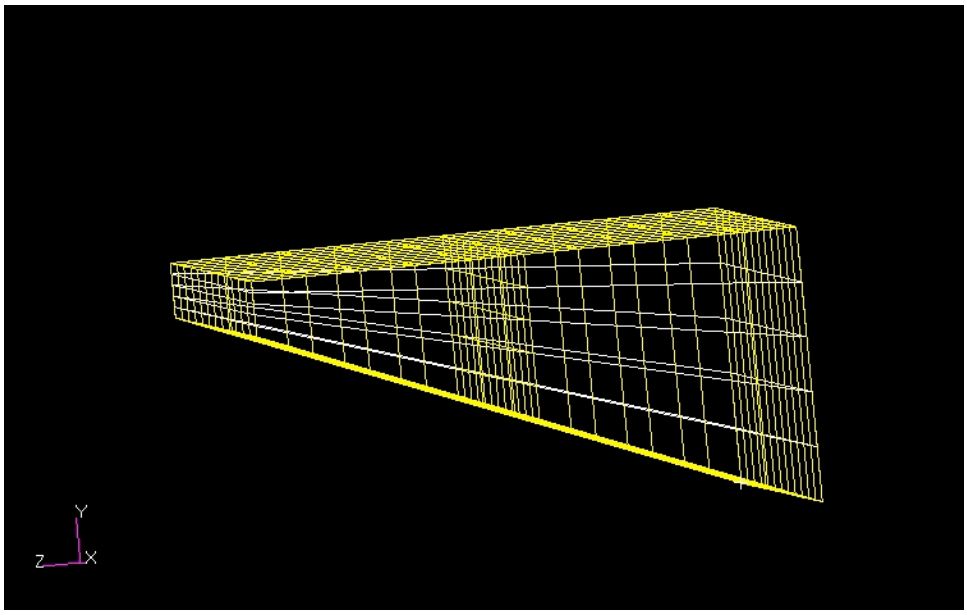

FIGURE 7: Wireframe of 10 m Model

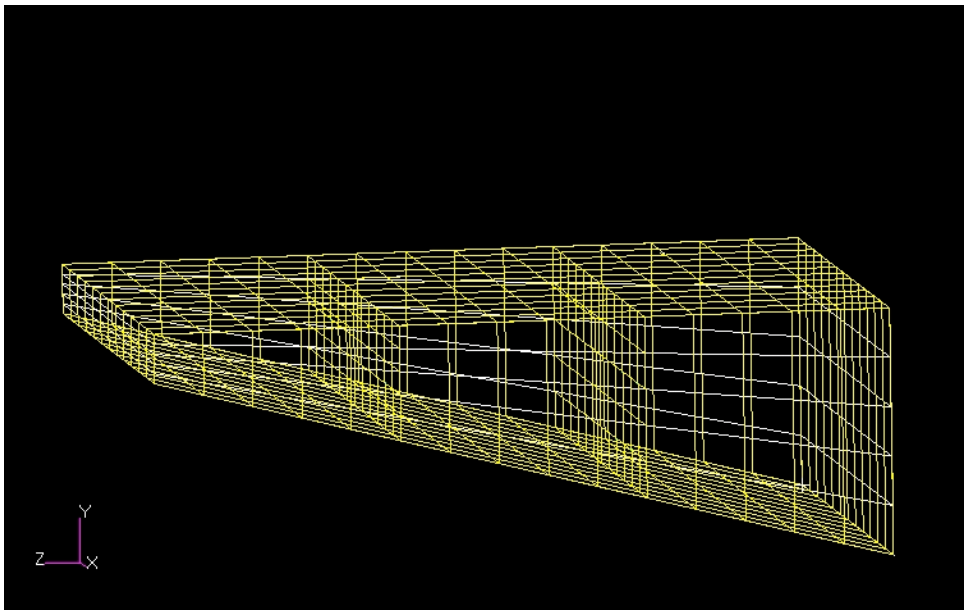

FIGURE 8: Wireframe of 15 m Model

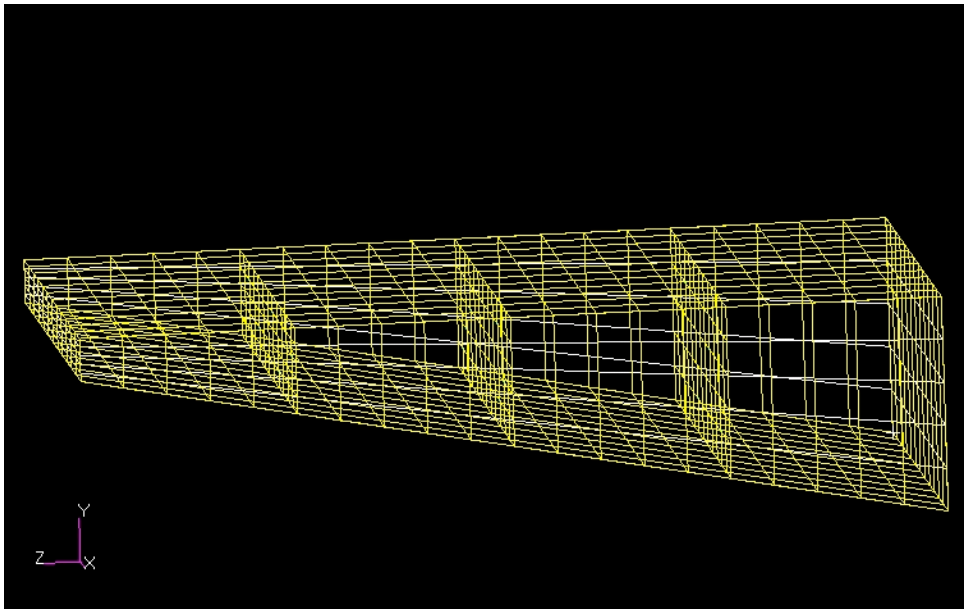

FIGURE 9: Wireframe of 20 m Model

2. Elements

To create a mesh on a surface, starting nodes called mesh seeds are placed along the edges of the surface. From these mesh seeds, PATRAN's automesh function interpolates between the nodes on the edges to place nodes on the surface, then creates the mesh by connecting the nodes. All models consist of only two types of elements, quad elements and bar elements, with the quad elements created by the automesh function while the bar elements are created by hand.

Mesh seeds are placed on all twelve edges of each tank. Seeds are placed every meter along the eight edges of the top and bottom sides. Five seeds are placed along the four vertical side edges, thus putting a seed every 0.2 meters along the two front edges and a seed every meter along the two back edges.

When quad elements are automatically generated from these seeds, the top and back sides both have 1-meter by 1-meter panels and the front has 0.2-meter by 1-meter panels. Because of the slope of the bottom, the panels on this side are not square.

Instead, the panels are each 1-meter wide with lengths between 1.02 to 1.08 meters, depending on the overall length of the tank. The side panels are all trapezoids 1 meter long with widths from 0.2 meters at the front to 1 meter at the back (see Figures 7 to 9).

Both the quad elements and bar elements are based on the thickness constraints of 6-ply Graphite Epoxy. The quad elements are 9.144e-4 m thick. The bar elements are all I-beam cross sections. All three segments of the cross section were 0.25 m wide and 9.144e-4 m thick. These thicknesses are later varied to allow for the stress in each element. An example is given in Figure 10.

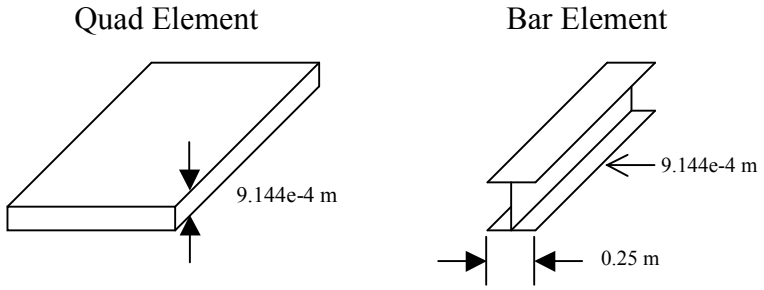

FIGURE 10: Example of Typical Panel and Bar Element

3. Materials

Two materials are considered in this analysis, although only one, Graphite Epoxy, is used in the models. The Graphite Epoxy used is IM/8552. It is analyzed as pseudo-isotropic and has a minimum thickness of 0.9144 mm. This minimum thickness comes from the requirement to wrap six plies per layer, each ply at 30 degrees, plus or minus 60 degrees (see Figure 11) and each ply 1.524e-4 m thick. The material properties are given in Table 3.

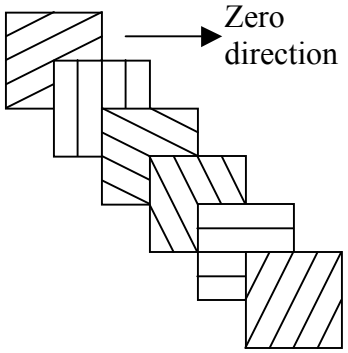

FIGURE 11 : Gr-Ep Lay-Up Scheme

TABLE 3: Graphite Epoxy Material Properties

PROPERTY	VALUE
E (Pa)	5.0332e10
ν	0.32
σ_{ult} (Pa)	7.24e8
ρ (kg/m3)	1799.2
Minimum thickness (m)	9.144e-4

The Aluminum-Lithium used is Al-Li 2097. This material is selected based on similar work conducted by the Boeing Company [2]. Because stress analysis depends on only geometry, applied loads, and boundary conditions, the stress results from the PATRAN/NASTRAN analysis using Gr-Ep are valid for any material. (Deflections, however, will be different for different materials; deflection is not considered in this analysis.) The different material properties that affects the final mass results are density and ultimate stress. Differences in these properties are accounted for in the data analysis stage. The material properties are given in Table 4.

TABLE 4: Aluminum Lithium Material Properties

PROPERTY	VALUE
E (Pa)	7.102e10
ν	0.32
σ_{ult} (Pa)	4.344e8
ρ (kg/m3)	2657.3
Minimum thickness (m)	2.5e-4

4. Loads and Boundary Conditions

Three types of loads are applied to the models: aerodynamic loads, nose loads, and interior pressure load. All of these loads are applied as distributed loads. Aerodynamic loads vary from a total of 1000 kN to 5000 kN, and are applied perpendicular to and into the bottom face of each model. Nose loads vary from 0 kN to 5000 kN, and are applied parallel to and point down from the front surface. Interior pressure loads are held constant at 2 atmospheres, or 202 kPa, and are assigned perpendicular to and out from all surfaces. The nose and aerodynamic loads are shown in Figure 12.

Two line boundary conditions are applied. The bottom edge of the back surface is restrained in all six degrees of freedom to provide a referent fixed point. The top edge of the back surface is constrained in four degrees of freedom, as it is allowed to translate along the y-axis (up and down) and rotate about the x-axis (pitch). This second boundary condition models the effect of the tank being joined at the back surface to the rest of a vehicle in flight rather than to a fixed surface. Both top and bottom line boundary conditions are shown in Figure 12.

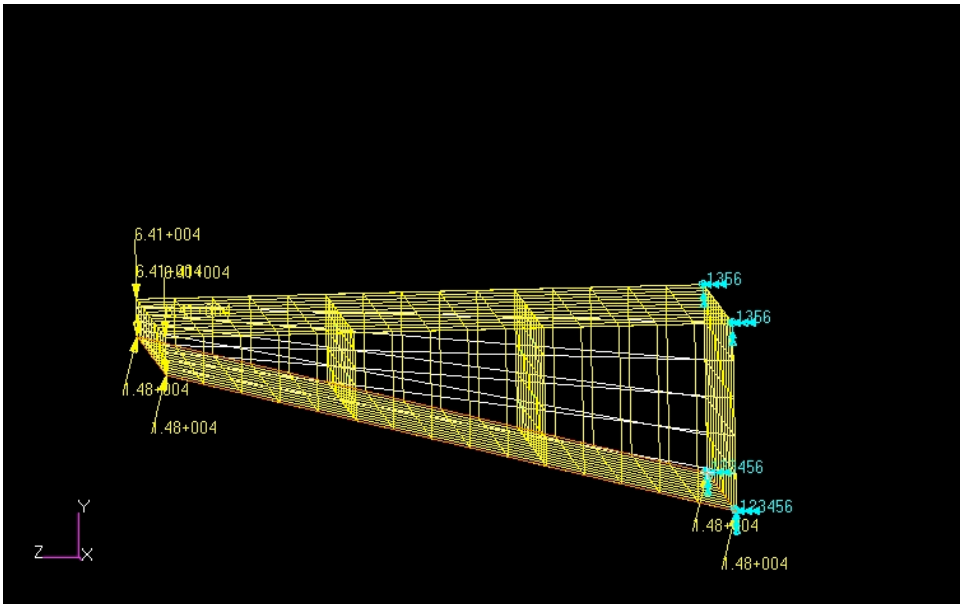

FIGURE 12: Loads and Boundary Conditions Applied to the 15 m Model

5. Stress Analysis

Once the model is completed and the appropriate load case is assigned, NASTRAN is run to calculate the stress in each element. This information is processed both computationally using Excel (see below) and graphically by PATRAN. An example of the stress contours for both quad and bar elements is given in Figures 13 and 14.

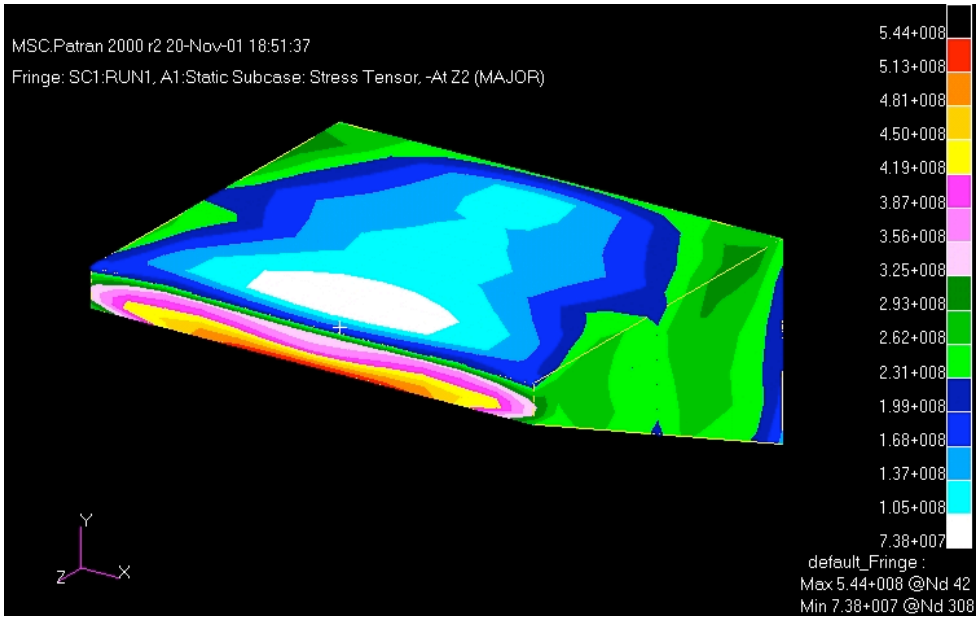

FIGURE 13: Generic Quad Element Stress Results

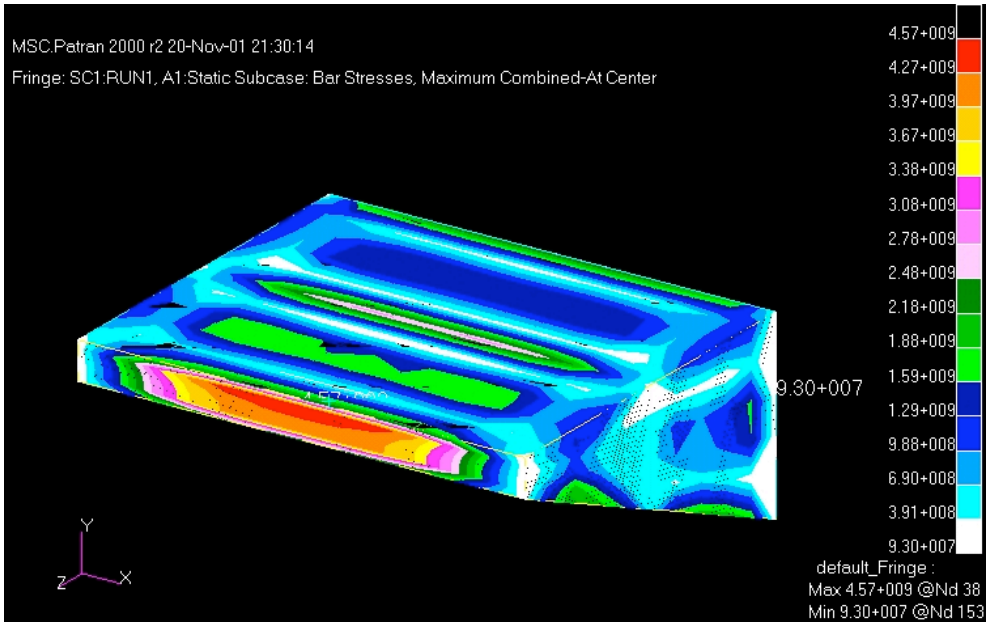

FIGURE 14: Generic Bar Element Stress Results

C. EXCEL

Data reduction and analysis is conducted using Excel spreadsheets. First the elemental stress data is parsed in bulk fashion from the .f06 NASTRAN output file then input into the data reduction worksheets. The two analysis worksheets, one for quad elements and one for bar elements, sample from these data reduction worksheets and then calculate the minimum allowed thickness for the stress in each element. This minimum thickness translates to a minimum mass for each element. Taking a sum over all the elements in the model gives the tank mass. After the tank masses for all the runs are collected, a Non-Optimum Factor (NOF) of an additional 20% is applied. The NOF accounts for difference between the simplified panel and bar model and the actual flight article. Finally, the MER is generated by regressing, using both Excel and Matlab, these modified results.

1. Data Reduction

Raw data taken from NASTRAN output is reduced to the applicable data by use of three separate worksheets. Raw data for quad element stress is read into a blank Excel workbook then copied into the Raw Quad Data worksheet or the Analysis workbook, seen in Figure 15. The Clean Quad Data worksheet is set up to select the maximum principal stress at the center of each element. This value is next sent to Quad Element Analysis sheet.

The Clean Bar Data worksheet is created by directly importing data from the NASTRAN .f06 file then applying a macro to remove extraneous text such as column headers. The worksheet selected the maximum bending stress seen in the element, and passed that information to the Bar Element Analysis worksheet.

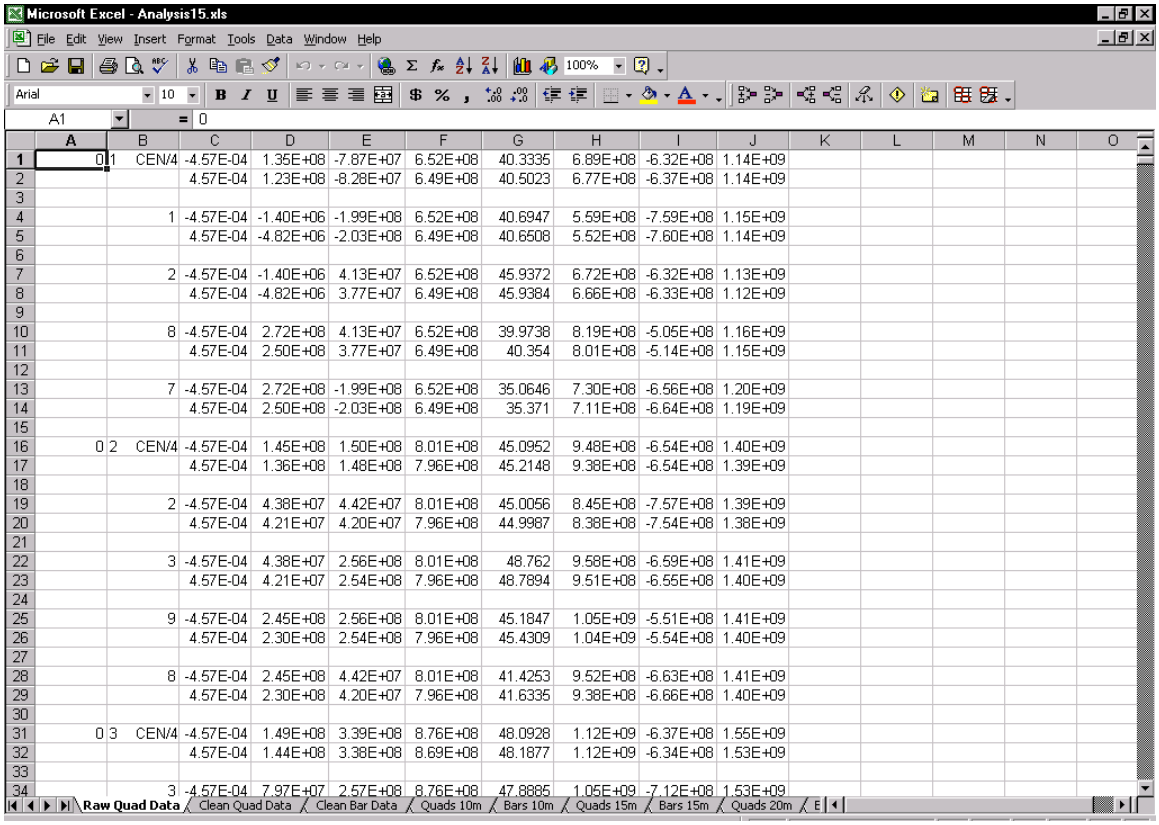

	A	B	C	D	E	F	G	H	I	J	K	L	M	N	O
1	0	1 CEN/4	-4.57E-04	1.35E+08	-7.87E+07	6.52E+08	40.3335	6.89E+08	-6.32E+08	1.14E+09					
2			4.57E-04	1.23E+08	-8.28E+07	6.49E+08	40.5023	6.77E+08	-6.37E+08	1.14E+09					
3															
4		1	-4.57E-04	-1.40E+06	-1.99E+08	6.52E+08	40.6947	5.59E+08	-7.59E+08	1.15E+09					
5			4.57E-04	-4.82E+06	-2.03E+08	6.49E+08	40.6508	5.52E+08	-7.60E+08	1.14E+09					
6															
7		2	-4.57E-04	-1.40E+06	4.13E+07	6.52E+08	45.9372	6.72E+08	-6.32E+08	1.13E+09					
8			4.57E-04	-4.82E+06	3.77E+07	6.49E+08	45.9384	6.66E+08	-6.33E+08	1.12E+09					
9															
10		8	-4.57E-04	2.72E+08	4.13E+07	6.52E+08	39.9738	8.19E+08	-5.05E+08	1.16E+09					
11			4.57E-04	2.50E+08	3.77E+07	6.49E+08	40.354	8.01E+08	-5.14E+08	1.15E+09					
12															
13		7	-4.57E-04	2.72E+08	-1.99E+08	6.52E+08	35.0646	7.30E+08	-6.56E+08	1.20E+09					
14			4.57E-04	2.50E+08	-2.03E+08	6.49E+08	35.371	7.11E+08	-6.64E+08	1.19E+09					
15															
16	0	2 CEN/4	-4.57E-04	1.45E+08	1.50E+08	8.01E+08	45.0952	9.48E+08	-6.54E+08	1.40E+09					
17			4.57E-04	1.36E+08	1.48E+08	7.96E+08	45.2148	9.38E+08	-6.54E+08	1.39E+09					
18															
19		2	-4.57E-04	4.38E+07	4.42E+07	8.01E+08	45.0056	8.45E+08	-7.57E+08	1.39E+09					
20			4.57E-04	4.21E+07	4.20E+07	7.96E+08	44.9987	8.38E+08	-7.54E+08	1.38E+09					
21															
22		3	-4.57E-04	4.38E+07	2.56E+08	8.01E+08	48.762	9.58E+08	-6.59E+08	1.41E+09					
23			4.57E-04	4.21E+07	2.54E+08	7.96E+08	48.7894	9.51E+08	-6.55E+08	1.40E+09					
24															
25		9	-4.57E-04	2.45E+08	2.56E+08	8.01E+08	45.1847	1.05E+09	-5.51E+08	1.41E+09					
26			4.57E-04	2.30E+08	2.54E+08	7.96E+08	45.4309	1.04E+09	-5.54E+08	1.40E+09					
27															
28		8	-4.57E-04	2.45E+08	4.42E+07	8.01E+08	41.4253	9.52E+08	-6.63E+08	1.41E+09					
29			4.57E-04	2.30E+08	4.20E+07	7.96E+08	41.6335	9.38E+08	-6.66E+08	1.40E+09					
30															
31	0	3 CEN/4	-4.57E-04	1.49E+08	3.39E+08	8.76E+08	48.0928	1.12E+09	-6.37E+08	1.55E+09					
32			4.57E-04	1.44E+08	3.38E+08	8.69E+08	48.1877	1.12E+09	-6.34E+08	1.53E+09					
33															
34		3	-4.57E-04	7.97E+07	2.57E+08	8.76E+08	47.8885	1.05E+09	-7.12E+08	1.53E+09					

FIGURE 15: Screenshot of Data Reduction Sheet

2. Quad Element Analysis

Quad elements analysis consists of one spreadsheet. For each quad element, it calculates the minimum thickness allowable based on the stress in the element, the ultimate stress of the material (divided by a factor of safety of 1.25), and the integer thickness of each layer. This thickness is combined with the area of the element and the density of the material to produce the mass of the element. Summing over all quad elements gives the minimum mass for the skin of the tank. An example of this worksheet is given in Figure 16.

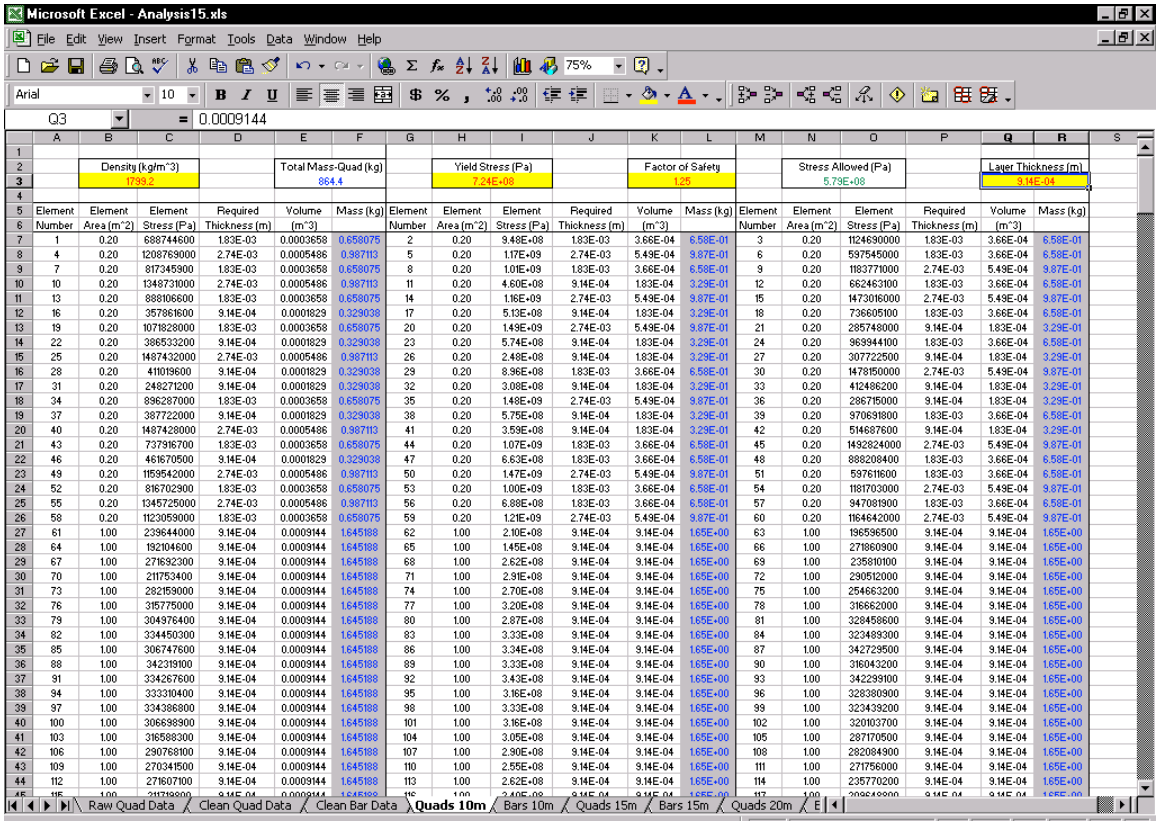

FIGURE 16: Screenshot of Quad Element Analysis Sheet

3. Bar Element Analysis

Bar Element analysis also consists of one spreadsheet. The stress in each bar element is assumed to be pure bending stress and that only the caps of the I-beam cross-section carry that stress, although the mass of the center web of the I-beam is included. The thickness of the caps is varied in order to vary the moment of inertia of the cross-section, while the thickness of the web is held constant at the minimum thickness of the material. The moment of inertia varies directly with the area of the cross-section (and hence varies directly with the thickness of the caps) and the distance of the cross-section from the neutral axis. Because changes in the thickness (approximately 0.0005 m) of the caps is relatively small compared to the distance to the neutral axis (approximately 0.125 m, see Figure 10), the fractional change in the distance from the neutral axis can be neglected. This leaves the moment of inertia proportional to the thickness of the caps. Thus, bending stress is inversely proportional with the thickness of those two plates.

Similar to the quad element analysis, a minimum thickness for each I-beam is calculated, based on the stress in the element, the ultimate stress of the material (divided by a factor of safety of 1.25), and the integer thickness of each layer. This thickness is combined with the area of the element and the density of the material to produce the mass of the element. Summing over all bar elements gives the minimum mass for the skeleton of the tank. An example of this worksheet is given in Figure 17.

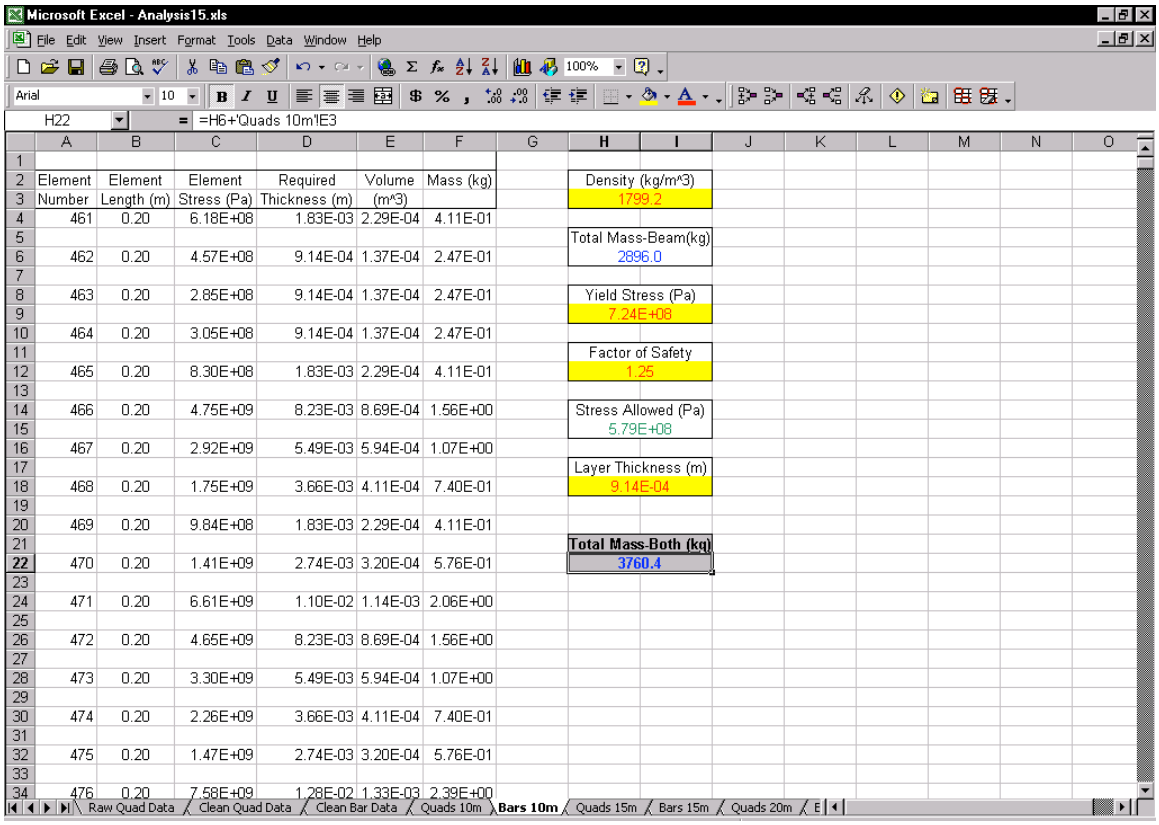

Microsoft Excel - Analysis15.xls

File Edit View Insert Format Tools Data Window Help

Arial 10 B I U 100%

H22 = =H6+'Quads 10m'!E3

	A	B	C	D	E	F	G	H	I	J	K	L	M	N	O
1															
2	Element	Element	Element	Required	Volume	Mass (kg)		Density (kg/m^3)							
3	Number	Length (m)	Stress (Pa)	Thickness (m)	(m^3)			1799.2							
4	461	0.20	6.18E+08	1.83E-03	2.29E-04	4.11E-01									
5								Total Mass-Beam(kg)							
6	462	0.20	4.57E+08	9.14E-04	1.37E-04	2.47E-01		2896.0							
7															
8	463	0.20	2.85E+08	9.14E-04	1.37E-04	2.47E-01		Yield Stress (Pa)							
9								7.24E+08							
10	464	0.20	3.05E+08	9.14E-04	1.37E-04	2.47E-01									
11								Factor of Safety							
12	465	0.20	8.30E+08	1.83E-03	2.29E-04	4.11E-01		1.25							
13															
14	466	0.20	4.75E+09	8.23E-03	8.69E-04	1.56E+00		Stress Allowed (Pa)							
15								5.79E+08							
16	467	0.20	2.92E+09	5.49E-03	5.94E-04	1.07E+00									
17								Layer Thickness (m)							
18	468	0.20	1.75E+09	3.66E-03	4.11E-04	7.40E-01		9.14E-04							
19															
20	469	0.20	9.84E+08	1.83E-03	2.29E-04	4.11E-01									
21								**Total Mass-Both (kg)**							
22	470	0.20	1.41E+09	2.74E-03	3.20E-04	5.76E-01		**3760.4**							
23															
24	471	0.20	6.61E+09	1.10E-02	1.14E-03	2.06E+00									
25															
26	472	0.20	4.65E+09	8.23E-03	8.69E-04	1.56E+00									
27															
28	473	0.20	3.30E+09	5.49E-03	5.94E-04	1.07E+00									
29															
30	474	0.20	2.26E+09	3.66E-03	4.11E-04	7.40E-01									
31															
32	475	0.20	1.47E+09	2.74E-03	3.20E-04	5.76E-01									
33															
34	476	0.20	7.58E+09	1.28E-02	1.33E-03	2.39E+00									

Raw Quad Data | Clean Quad Data | Clean Bar Data | Quads 10m | **Bars 10m** | Quads 15m | Bars 15m | Quads 20m | E

FIGURE 17: Screenshot of Bar Element Analysis Sheet

IV. RESULTS

Once the mass of each tank is known for each run, it is possible to generate a RSE that would serve as an MER.

A. Generation of 6-ply Graphite Epoxy MER

The results of each separate Excel worksheet for the individual runs of the DOE are collected into another spreadsheet, and given in Table 5. The results given in Table 5 come directly from the results of the analysis, and do not include the NOF.

TABLE 5: Tank Masses for each run, using 6-ply Gr-Ep

Run	Length (m)	Aero Load (kN)	Nose Load (kN)	Tank mass (kg)
1	10	2000	0	3270.6
2	10	2000	5000	3766.3
3	10	4000	0	3122.1
4	10	4000	5000	3485.4
5	20	2000	0	5827.6
6	20	2000	5000	6921.2
7	20	4000	0	5934.0
8	20	4000	5000	6696.8
9	15	3000	2500	4587.9
10	10	3000	2500	3321.8
11	20	3000	2500	6027.9
12	15	1000	2500	4931.5
13	15	5000	2500	4546.8
14	15	3000	2500	4439.6
15	15	3000	5000	5121.0

Matlab is then used to estimate the MER coefficients, followed by using Excel with Solver to ensure that the fit of the regression has the minimum error. The following RSE is generated, yielding the MER for 6-ply Graphite Epoxy.

$$M = (1862.3 + 154.3\ L - 0.351\ A - 0.0838\ N + 0.00797\ LA + 0.00100\ LN - 0.000023\ AN + 2.853\ L^2 + 0.0000345\ A^2 + 0.0000278\ N^2) * (1 + NOF)$$

Where M is tank mass in kg, L is tank length in m, A is aerodynamic load in kN, and N is tank nose load in kN. This surface is best displayed in three dimensions, although there

are four variables (three independent and one dependent). Thus A is held constant in the following two figures. The MER is shown with A set equal to 1000 kN in Figure 18, and with A=5000 kN in Figure 19.

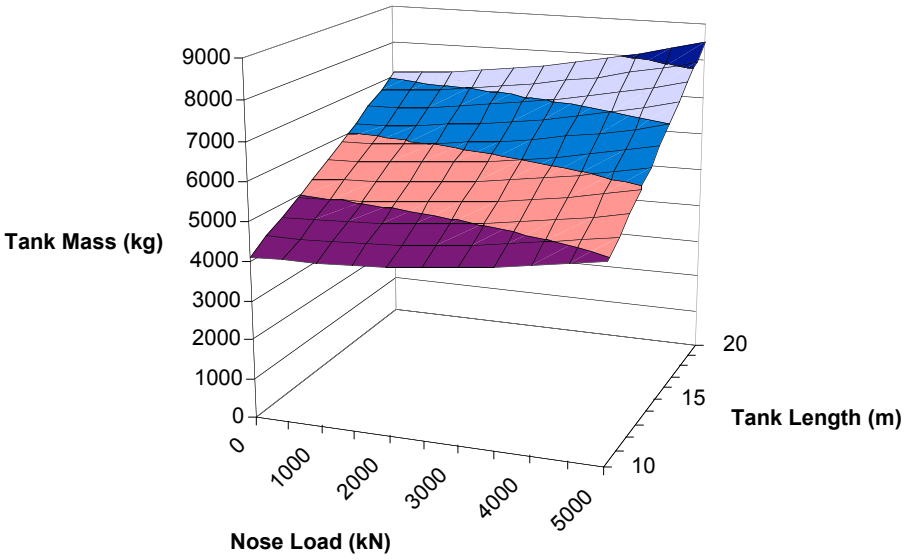

FIGURE 18: Marcus for 6-ply Gr-Ep, with A = 1000 kN

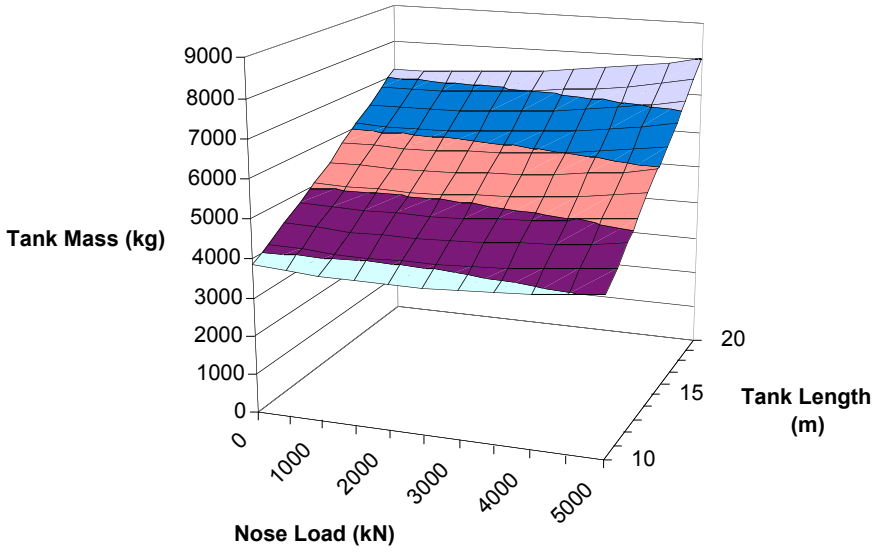

FIGURE 19: Marcus for 6-ply Gr-Ep, with A = 5000 kN

A one-variable-at-a-time analysis of this MER is given in Data Analysis. It gives a numerical evaluation of the general trend of the RSE about the central point of the DOE.

B. Generation of 3-ply Graphite Epoxy MER

Based on the stress results from the 6-ply Graphite Epoxy, it is assumed that the stress is perfectly inversely proportional with thickness. Thus, the stress results from using 6-ply Gr-Ep could be concentrated in a 3-ply Graphite Epoxy thickness by simply applying a factor of 2. This new higher stress would be analyzed similar to the way the 6-ply data was analyzed in order to find out how much mass was saved by cutting the incremental thickness in half. The mass results of this analysis, without applying the NOF, are given in Table 6.

TABLE 6: Tank Masses for each Run, using 3-ply Graphite Epoxy

Run	Length (m)	Aero Load (kN)	Nose Load (kN)	Tank mass (kg)
1	10	2000	0	2726.0
2	10	2000	5000	3293.0
3	10	4000	0	2561.3
4	10	4000	5000	2966.3
5	20	2000	0	4742.3
6	20	2000	5000	5974.0
7	20	4000	0	4945.9
8	20	4000	5000	5729.7
9	15	3000	2500	3726.6
10	10	3000	2500	2814.0
11	20	3000	2500	5080.6
12	15	1000	2500	4203.4
13	15	5000	2500	3802.2
14	15	3000	2500	3625.7
15	15	3000	5000	4375.5

$$M = (1954.3 + 84.4\,L - .380\,A - .0231\,N + .0113\,LA + .0104\,LN$$
$$- .0000304\,AN + 3.264\,L^2 + .0000339\,A^2 + .0000216\,N^2) * (1 + NOF)$$

Where M is tank mass in kg, L is tank Length in m, A is aerodynamic load in kN, and N is tank nose load in kN. This surface is shown, with A = 1000 kN, in Figure 20.

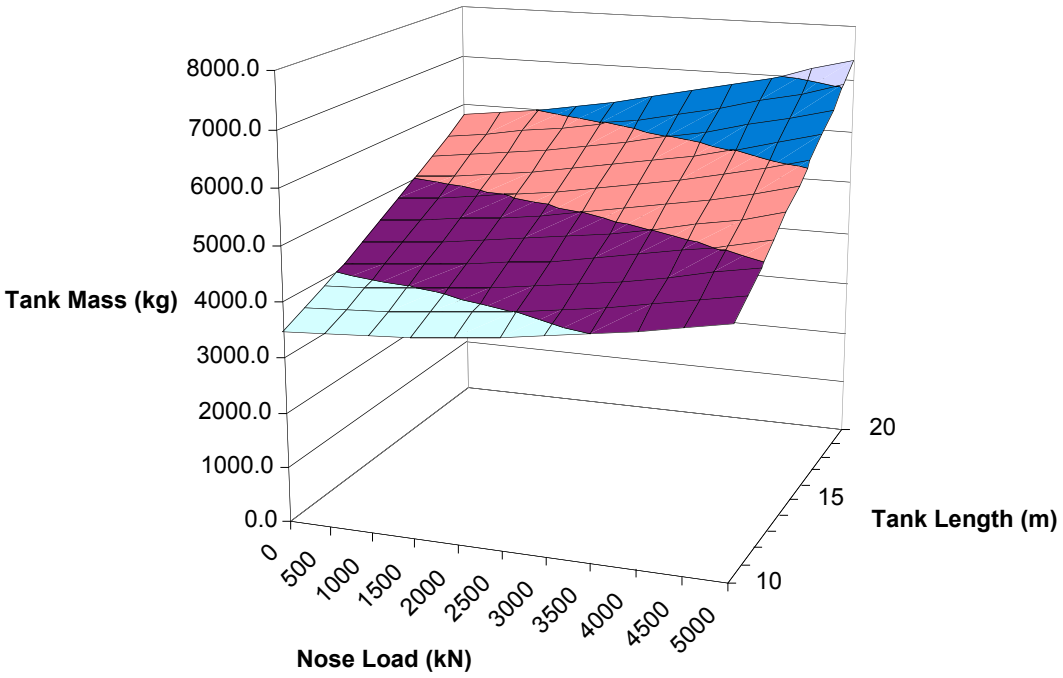

FIGURE 20: Marcus for 3-ply Gr-Ep, with A = 1000 kN

C. Generation of Aluminum-Lithium MER

This analysis is also conducted based on the stress results of the 6-ply Graphite Epoxy models. As previously discussed in the Materials section, the stress results are the same for 6-ply Gr-Ep as for Al-Li. However, the stress results do need to be adjusted for the change in the minimum allowable thickness. This is completed in the same manner as the stress results are adjusted for 3-ply Gr-Ep, by concentrating the stress into the new smaller thickness. Additionally, the analysis allows for continuously variable thickness, subject to the minimum allowable thickness. Results of this analysis, not including the NOF, are given in Table 7.

TABLE 7: Tank Masses for each run, using Al-Li

Run	Length (m)	Aero Load (kN)	Nose Load (kN)	Tank mass (kg)
1	10	2000	0	5734.2
2	10	2000	5000	7147.4
3	10	4000	0	5310.8
4	10	4000	5000	6290.2
5	20	2000	0	9852.8
6	20	2000	5000	12754.8
7	20	4000	0	10368.5
8	20	4000	5000	12142.8
9	15	3000	2500	7623.6
10	10	3000	2500	5971.4
11	20	3000	2500	10676.0
12	15	1000	2500	8892.1
13	15	5000	2500	7898.7
14	15	3000	2500	7572.5
15	15	3000	5000	9304.3

$$M = (5736.0 + 8.379\ L - 1.138\ A - .0831\ N + .0296\ LA + .0228\ LN$$
$$- .0000781\ AN + 11.75\ L^2 + .000113\ A^2 + .0000654\ N^2) * (1+ NOF)$$

Where M is tank mass in kg, L is tank length in m, A is aerodynamic load in kN, and N is tank nose load in kN. This surface is shown, with A = 1000 kN, in Figure 21.

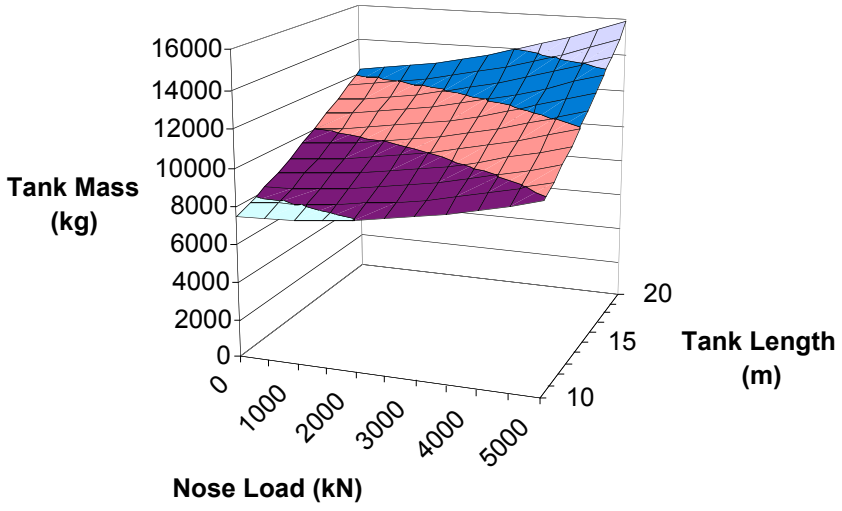

FIGURE 21: Marcus for Al-Li, with A = 1000 kN

V. ANALYSIS OF RESULTS

With the MERs now available to use, comparison can be made with the LOX Factor, as applied to a traditionally created MER, in this case one taken from the Brothers database from the Marshall Space Flight Center (MSFC)[3]. But first, a representative physics-based MER is evaluated to ensure it follows the "common sense" test.

A. Analysis of Marcus 6-ply Gr-Ep MER

This one variable at a time analysis is conducted to numerically show that while some of the linear terms of the MER are negative, the general trend of tank mass is reasonable. The analysis is conducted about the center point of the DOE, where L = 15 m, A = 3000 kN, and N = 2500 kN. Taking partial derivatives yields:

$$\frac{\partial M}{\partial L} = (154.3 + 0.00797A + 0.001N + 5.706L) * (1.2) = 319.56$$

$$\frac{\partial M}{\partial A} = (-0.351 + 0.00797L - 0.000023N + .000069A) * (1.2) = -0.098$$

$$\frac{\partial M}{\partial N} = (-0.0838 + 0.001L - 0.000023A + .0000556N) * (1.2) = 0.00144$$

Thus, for a one meter increase in tank length, tank mass should go up about 320 kg; for a 1000 kN increase in aerodynamic load, tank mass should go down by 98 kg; for a 1000 kN increase in nose load, tank mass should go up by 1.44 kg.

This is easy to see in Figure 18, where most of the curvature occurs with variation along the length axis. The negative dependence on aerodynamic load is understandable because at that value of aerodynamic load, it helps to reduce the overall effect of the interior pressure and the aerodynamic load taken together.

B. Analysis of Brothers MER, With and Without the LOX Factor Applied

The historical-based MER used for comparison comes from the Brothers MER database from MSFC. Translated into metric and the terms of this research, the MER is:

$$M = 1.09 * (1293.7L)^{0.85653}$$

Where M is tank Mass in kg and L is tank Length in m. As can be seen from the above equation, this MER depends only on the geometry of the tank, in this case simply the length of the tank. The results of this MER are given in Figure 22.

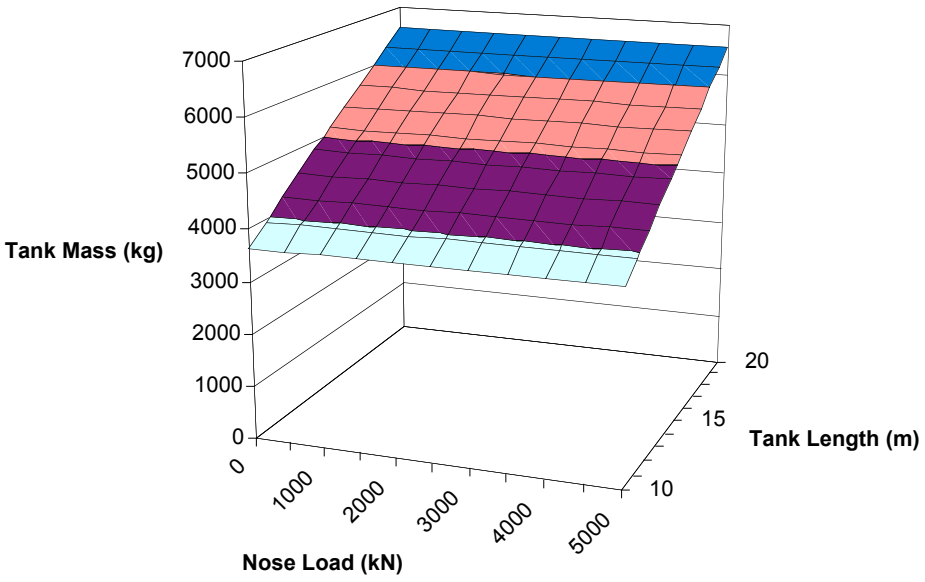

FIGURE 22: Brothers MER

The proposed solution for the problem of the LOX tank bending loads is given earlier in Figure 5. The equation given in Figure 5 uses the variable of Density Ratio (DR = ρ_{prop} / ρ_{ref}) without specifying the components of ρ_{prop}. In order to compare the LOX Factor with the results of this research, assumptions are made concerning ρ_{prop}. First, that ρ_{prop} is calculated as the total propellant mass divided by the total propellant volume. Second, that the mass of the LOX is equal only to the Nose Load divided by 2.5

g's. Third, that the volume of the LH_2 tank is completely full of fuel. Fourth, that the forward LH_2 tank and the forward LOX tanks are the only sources of propellant considered for calculating $\square_{prop}$ (e.g. mass of propellant in any aft tanks is ignored). Based on these assumptions the Density Ratio, and thus the LOX Factor, translates into metric and the terms of this research as:

$$DR = \frac{40.82N + 2556L}{5.47N + 5508L}$$

$$LOX\_Factor = 0.682 + 0.272DR + 0.046DR^2$$

The LOX Factor as it is applied to the Brothers MER is shown in Figure 23.

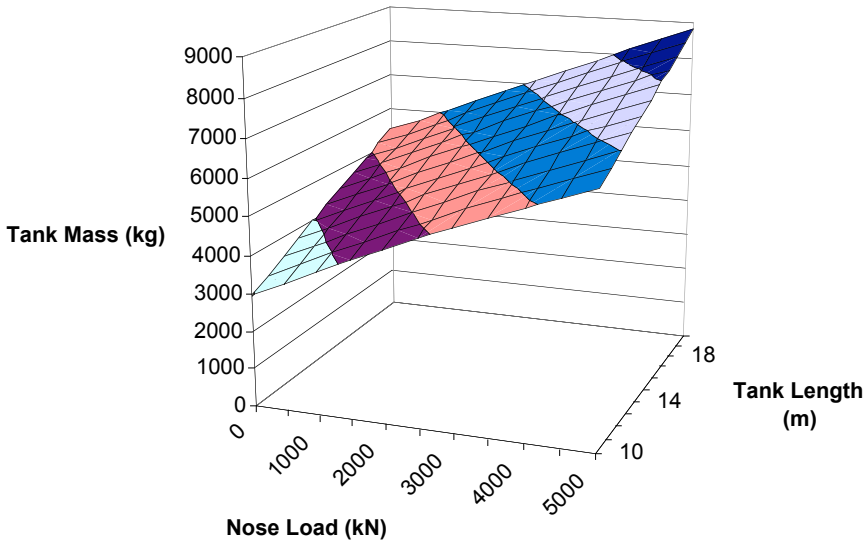

FIGURE 23: Brothers MER with the LOX Factor Applied

C. Analysis of Different MERs, with Nose Load and Aero Load Held Constant

The three different MERs (Marcus, Brothers, and Brothers w/LOX Factor) are shown in Figure 24 and Figure 25. In both figures, aerodynamic load is held at the minimum value of the DOE, 1000 kN.

In Figure 24, nose load is at its minimum value of zero. The Marcus MER is about 20% more than the Brothers MER (the amount of the NOF) and about 40% more than the Brothers MER with the LOX Factor applied. However, as the NOF is not yet well defined, the most important thing to consider is that the trend of all three lines is very similar, almost to the point of the three being parallel.

In Figure 25, nose load is at its maximum value of 5000 kN, and while the general trend of all three lines is the same, the ordering has changed. The Brothers MER with the LOX Factor applied is 40% more than the Marcus MER and 85% more than the Brothers MER by itself. But again, the trend between the two lines is similar, leading to the conclusion that by judicial use of the NOF, the physics-based MER and the LOX Factor can be brought into agreement with regard to variation relative to tank length. Nose load is a different situation, as seen by the drastic change in tank mass over the range of values for nose load.

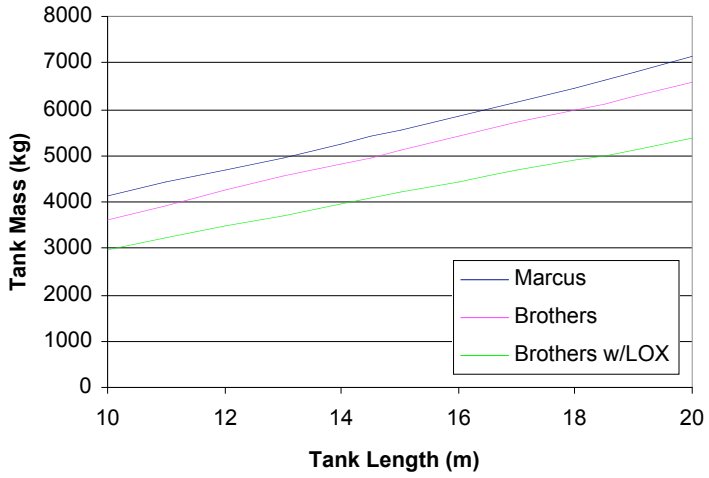

FIGURE 24: Tank Mass versus Tank Length (A = 1000 kN, N = 0 kN)

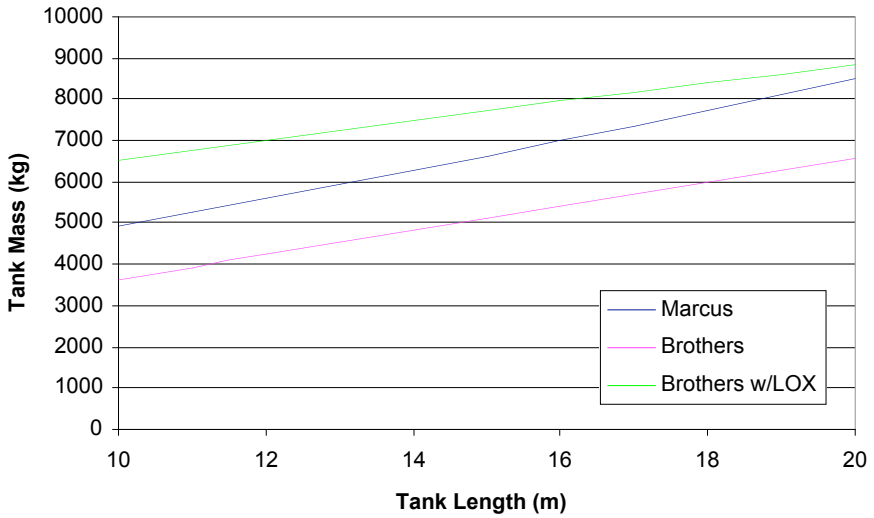

FIGURE 25: Tank Mass versus Tank Length (A = 1000 kN, N = 5000 kN)

D. Analysis of Different MERs, with Length and Aero Load Held Constant

The three different MERs (Marcus, Brothers, and Brothers w/LOX Factor) are shown in Figure 26 and Figure 27. In both figures, aerodynamic load is held at the minimum value of the DOE, 1000 kN.

In Figure 26, tank length is at its minimum value of 10 m. It is here that the difference between the physics-based MER and the LOX Factor is most evident, with the LOX Factor results varying by 120% of its value over the range of nose load, while the physics-based results only varied by about 20% of its value. And, as the shape of the two curves is different, the LOX Factor is almost linear with respect to nose load while the physics-based results show some small curvature, due to the effect of the cross and quadratic terms in the MER.

In Figure 27, tank length is at its maximum value of 20 m. And while not as pronounced as in Figure 26, the same general trend is shown, as the LOX Factor results

vary almost linearly up to 65% of its value, while the physics-based results vary only about 20% of its value. Further proof that the LOX Factor's variation with respect to nose load is inaccurate.

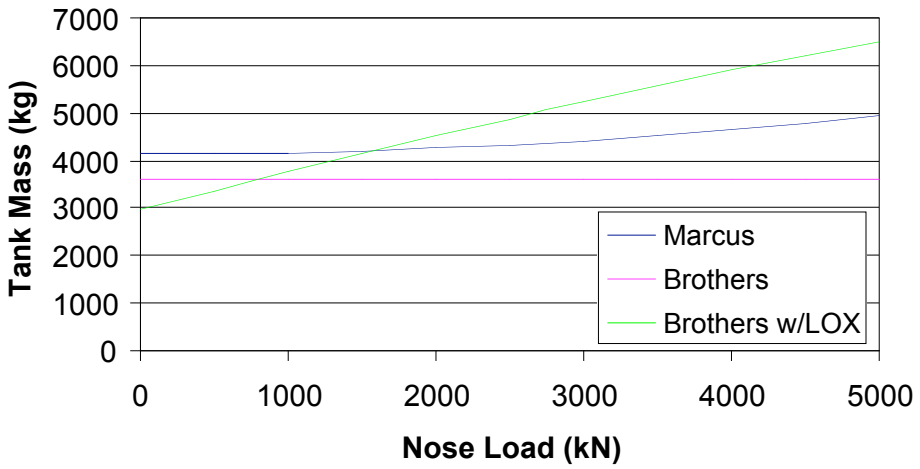

FIGURE 26: Tank Mass versus Nose Load (A = 1000 kN, L = 10 m)

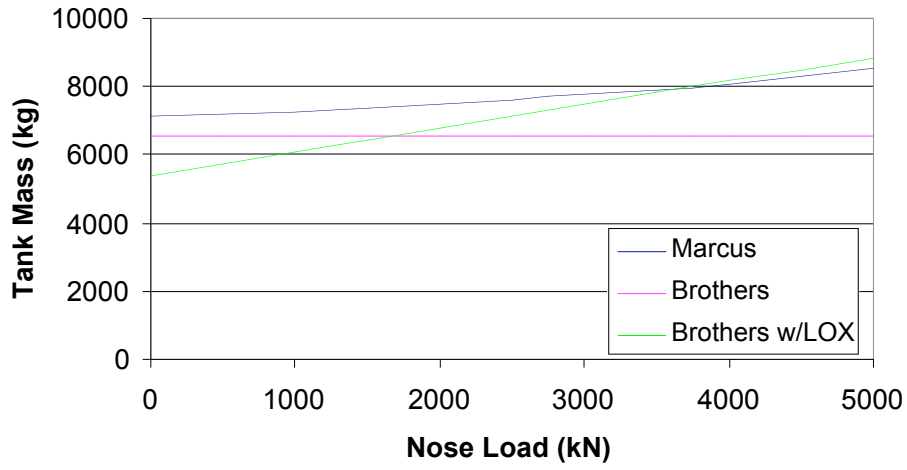

FIGURE 27: Tank Mass versus Nose Load (A = 1000 kN, L = 20 m)

VI. CONCLUSIONS AND FUTURE WORK

This research has two fundamental conclusions. The first is that while the LOX Factor is acceptable in terms of its variation with regard to tank length, it is probably overly aggressive with its variation with regard to nose load. This is most obvious in the way the LOX Factor predicts an almost 120% increase in tank mass when the physics-based MER predicts only a 20% (see Figure 26). However, as the comparison with the LOX Factor was based on a number of different assumptions, it is possible that that 120% increase does not accurately reflect the LOX Factor.

Secondly, this research shows that FEM can be successfully integrated into conceptual space vehicle design, although it is still significantly time consuming. Perhaps the next step in this development is the creation of an automatic capability to generate a geometry, assign design variables to it, run a simplified panel and bar element analysis, and then generate a MER from those results. With a rapid design tool available, the NOF could be accurately estimated by fine-tuning the tool until it returned known masses back for historical tanks. This capability would allow major structural components, most notably tanks and wings, to be mass estimated with a much higher degree of fidelity, in turn yielding a conceptual design of much higher accuracy.

VII. ACKNOWLEDGEMENTS

I would like to thank the following people for their support during the rather extended duration of this project: Dr. John Olds of Georgia Tech for his guidance and insight; Mr. Norman Brown and Mr. D.R. Komar of MSFC; and Dr. Michael Conley of AeroAstro for providing the use of PATRAN/NASTRAN and Mr. Robert Minelli of AeroAstro for lending his expertise in FEM.

VIII. REFERENCES

1. "Airbreathing Launch Vehicle Study Status Overview", presented by J.L. Hunt and D. H. Petley, NASA LaRC, at JANNAF, 10/99

2. "NASA Reference Vehicle – HXF-Ref1-B1", presented by D. Johnson and B. Bachinger, Boeing St. Louis, at NASA MSFC, 7/00

3. "Spacecraft Mass Estimating Relationship Database", by Bobby Brothers developed under contract to NASA MSFC, 2000. Database derived primarily from expendable vehicles and the Space Shuttle. Some equations are taken from AVID, a sizing code developed by A. W. Wilhite at NASA LaRC.

APPENDIX A

Additional Analysis

COMPARISON WITH CURRENT VEHICLE CONCEPTS

The LH_2 tanks of two RLV concepts previously analyzed by SSDL are considered using the MER for 6-ply and 3-ply Gr-Ep. These two vehicles are the ABLV-GT and Stargazer, and their LH_2 tank data are given in Table 8.

Table 8: Comparison of Fuel Tank Data

Vehicle Name	Tank Volume (m^3)	Equivalent Length (m)	Aero Load (kN)	Nose Load (kN)
ABLV-GT	692.36	19.23	1800	0
Stargazer	298.78	8.30	353	0

Tank volumes are taken directly from the Weights & Sizing sheets for each concept. Because the ABLV-GT had a forward and aft fuel tank, the forward fuel tank volume is taken as 50% of the overall tank volume.

The equivalent length is found based on the tank volume. When creating the MERs, three tank geometries are considered. Each was 12 m wide with a trapezoidal cross section having a 1 m high front panel and a 5 m high back panel. This left the length as the only geometric variable, resulting in a volume given by:

$$\text{Volume} = (12\text{ m})*[(0.5)*(1\text{ m} + 5\text{ m})]*(\text{Length})$$
$$\text{Volume} = (36\text{ m}^2) * (\text{Length})$$

Converting this into an equation for length in terms of volume yields:

$$\text{Length}_{\text{equiv}} = \text{Volume} / (36\text{ m}^2)$$

This measure is appropriate for both vehicles, as their fuel tanks are of similar geometry.

Aerodynamic load is based on whether the vehicle had significant lift developed from the bottom surface of the fuel tank, and is expressed as a total load, rather than a pressure. This total load is estimated as 60% of the vehicles' Gross Lift-Off Weight

(GLOW). However, as the ABLV-GT has a forward and aft fuel tank carrying this load, only half the total load, or 30% of the GLOW, is applied to the forward tank. Stargazer has only one tank. Thus, the entire load (60% of GLOW) is applied to that tank.

Neither vehicle has any significant amount of equipment forward of the LH_2 tank, and as such no nose load is assigned to either of these concepts.

These three characteristics for each tank were then entered into the two Gr-Ep MERs derived by this research. The resulting tank masses, including a 20% Non-Optimum Factor, are given in Table 9, with the tank mass from the original analysis.

Table 9: Comparison of Tank Mass Results

Vehicle Name	Original Mass (kg)	6-ply MER Mass (kg)	3-ply MER Mass (kg)
ABLV-GT	8400	6768	5484
Stargazer	1972	3892	3336

Interestingly, both MERs returned masses that are lighter for the ABLV-GT and heavier for Stargazer. However, Stargazer was outside the range of both Tank Length (10 m to 20 m) and Aerodynamic Load (1000 kN to 5000 kN) used in the DOE that generated both MERs. This is one significant reason for the MER to be heavy for Stargazer. Another effect to consider is that both Stargazer and ABLV-GT have internal tank pressures of 2 atmospheres absolute, while the cases in the DOE have internal tank pressure of 3 atmospheres absolute. This difference is analyzed in the next section.

VARYING INTERNAL TANK PRESSURE

One additional run of FEA is conducted at the same conditions as Run 9, with the exception that the internal tank pressure is 2 atmospheres absolute, resulting in a one-atmosphere gage internal pressure load. The stress result plots are given in Figure 37 in Appendix B, along with stress plots for all other runs. The maximum stress experienced for both runs and the resulting tank masses are given in Table 10.

Table 10: Comparison of Element Stresses and Tank Masses

Run	Max Bar Element Stress (MPa)	Max Quad Element Stress (MPa)	6-ply MER Mass (kg)	3-ply MER Mass (kg)
9	5330	994	4588	3727
9a	3020	715	3244	2357

While the stress distributions are not identical (see Figures 36 and 37), they are similar enough to allow for an analysis based solely on maximum stress. As the variation in maximum stress (average reduction of 35%) and variation in the tank mass (average reduction of 33%) track almost exactly, it is reasonable to conclude that most elements are not at the minimum gage design condition. Since stress and element thickness are directly related in this research, if a significant number of elements reached minimum gage when internal pressure was reduced to two atmosphere, then the tank mass would "bottomed out" rather than been linearly related. From the magnitude of the change, internal pressure is an important input into determining tank mass; in future research, it will be included as an independent variable.

As previously noted, this research only considered two design conditions, which are: maximum allowable tensile stress and minimum gage thickness. If other design criteria and failure modes are considered (such as buckling or maximum allowable displacement) additional structural elements designed to prevent these other failure modes must be added. Mass estimating is affected by two competing effects associated with these additions. The first effect is simply that adding extra structure simply adds extra mass. However, this additional structure allows for a different load path, which could conceivably reduce stress in other members to the point that their mass is reduced. An example of this is shown by the tank construction using a skeleton of beam elements and a skin of panel elements. Had the tank been constructed simply of skin elements, the tank mass would have been two orders of magnitude greater. As with analyzing for the effect of internal pressure, future research will include analysis of additional failure modes.

APPENDIX B

All PATRAN Stress Plots

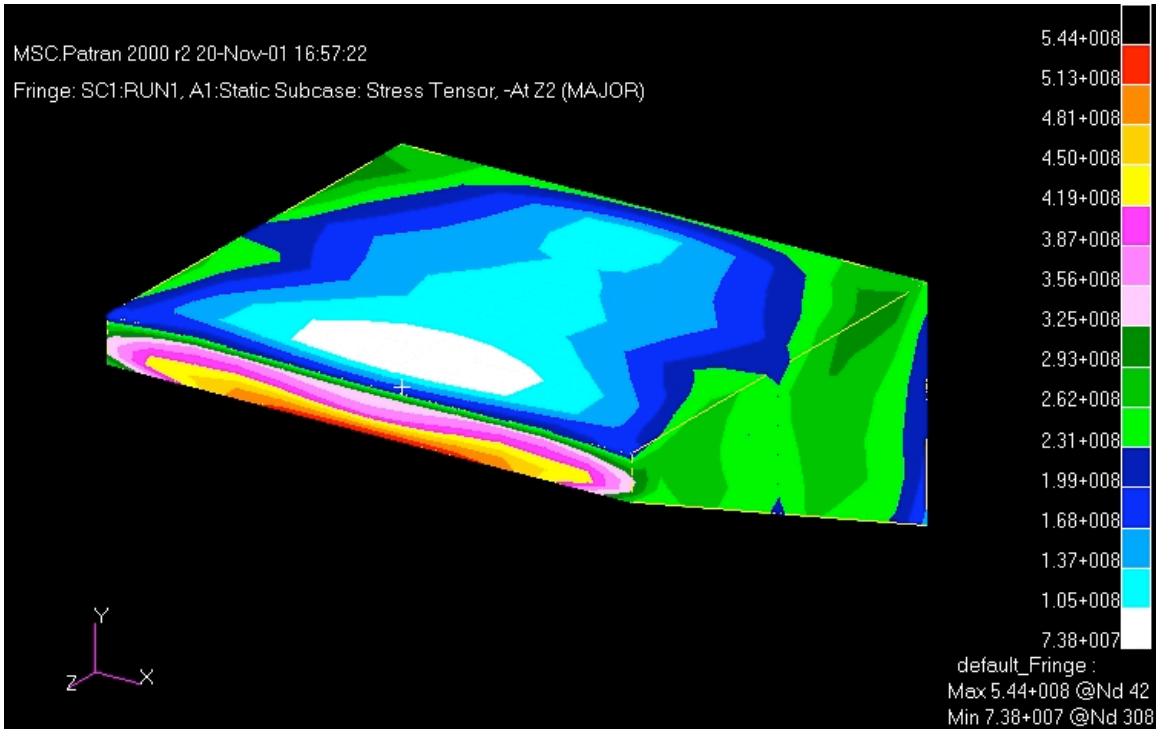

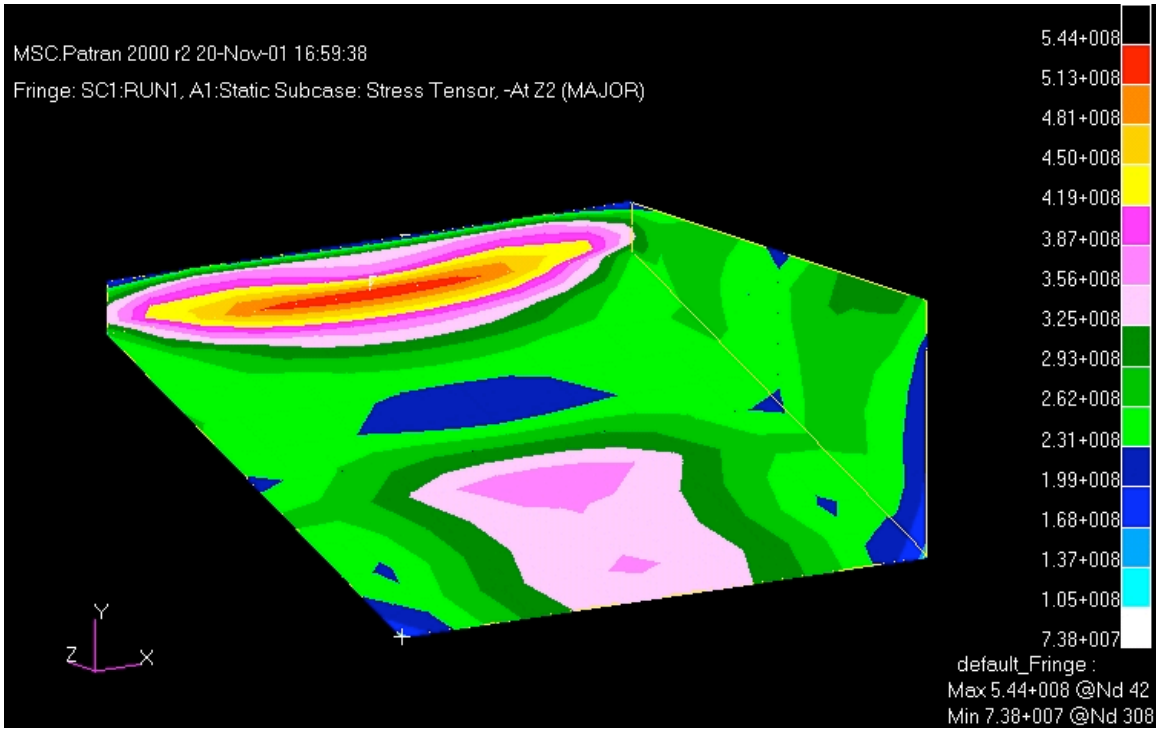

Figure 28: Stress Results for Run 1 (Stress in Pa)

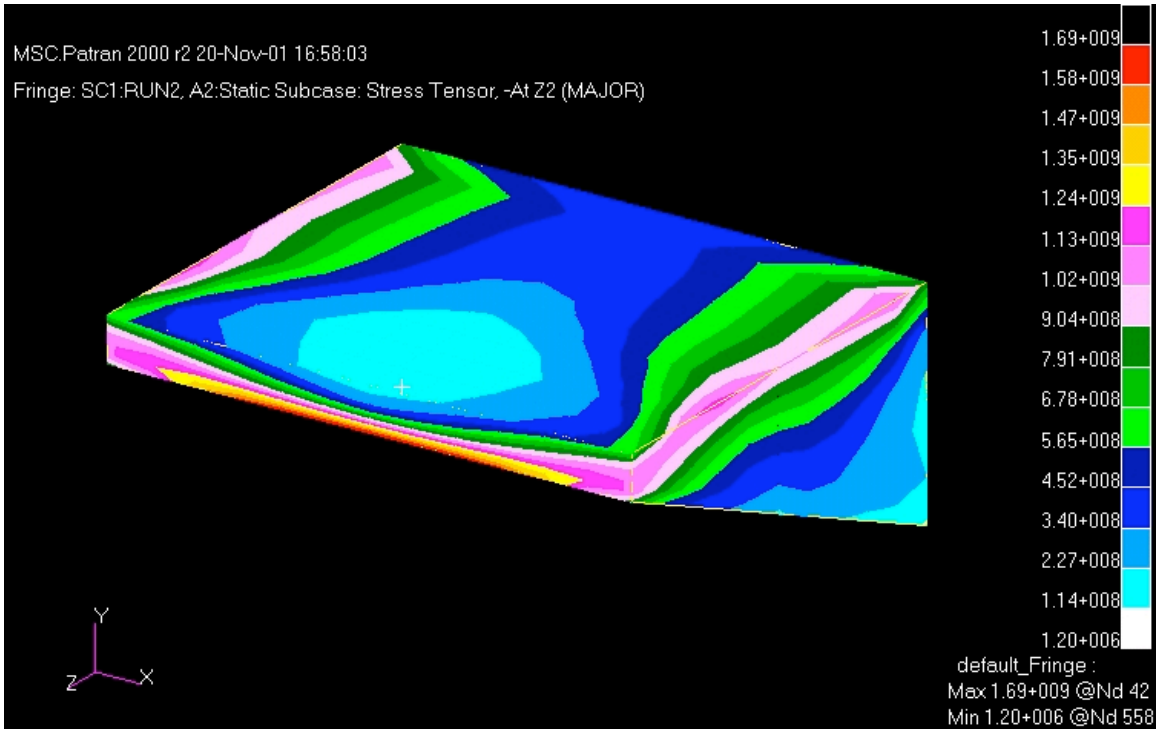

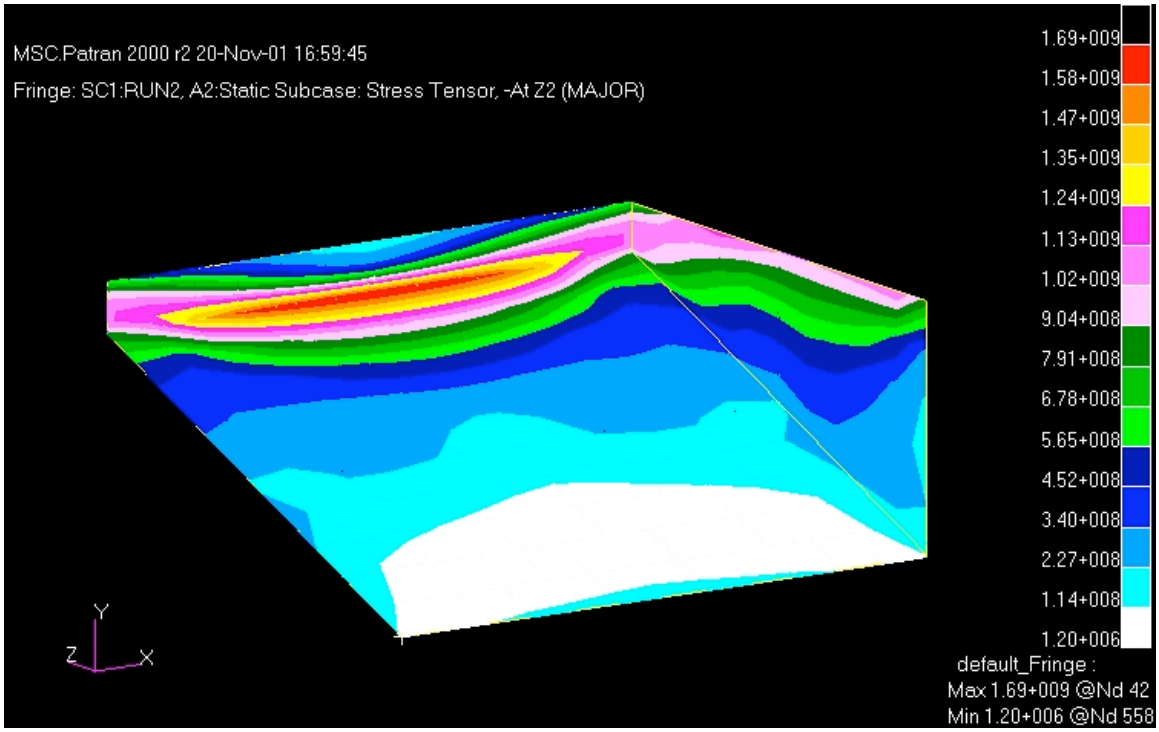

Figure 29: Stress Results for Run 2 (Stress in Pa)

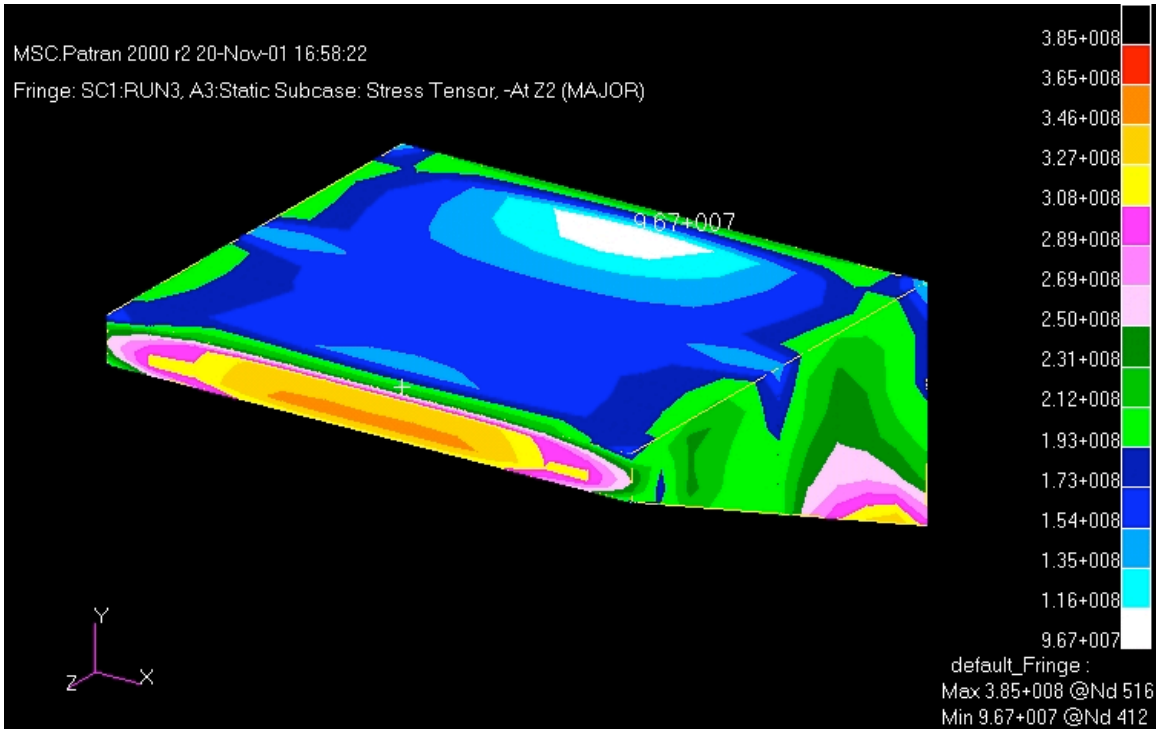

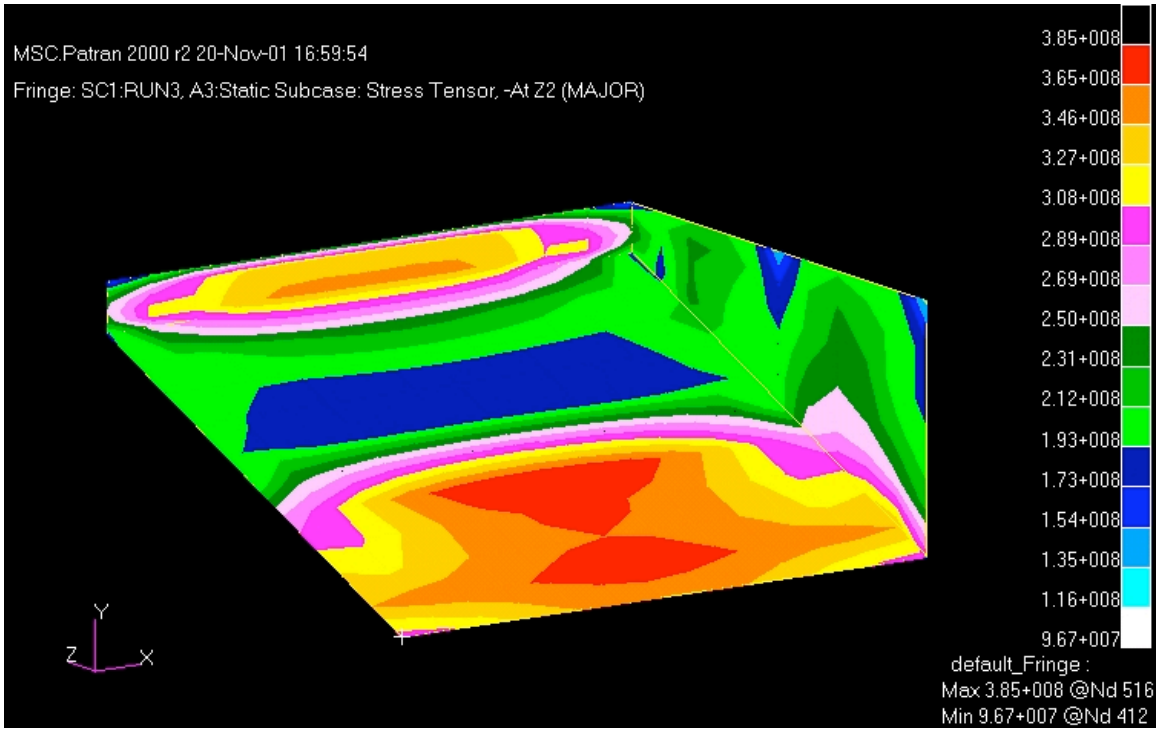

Figure 30: Stress Results for Run 3 (Stress in Pa)

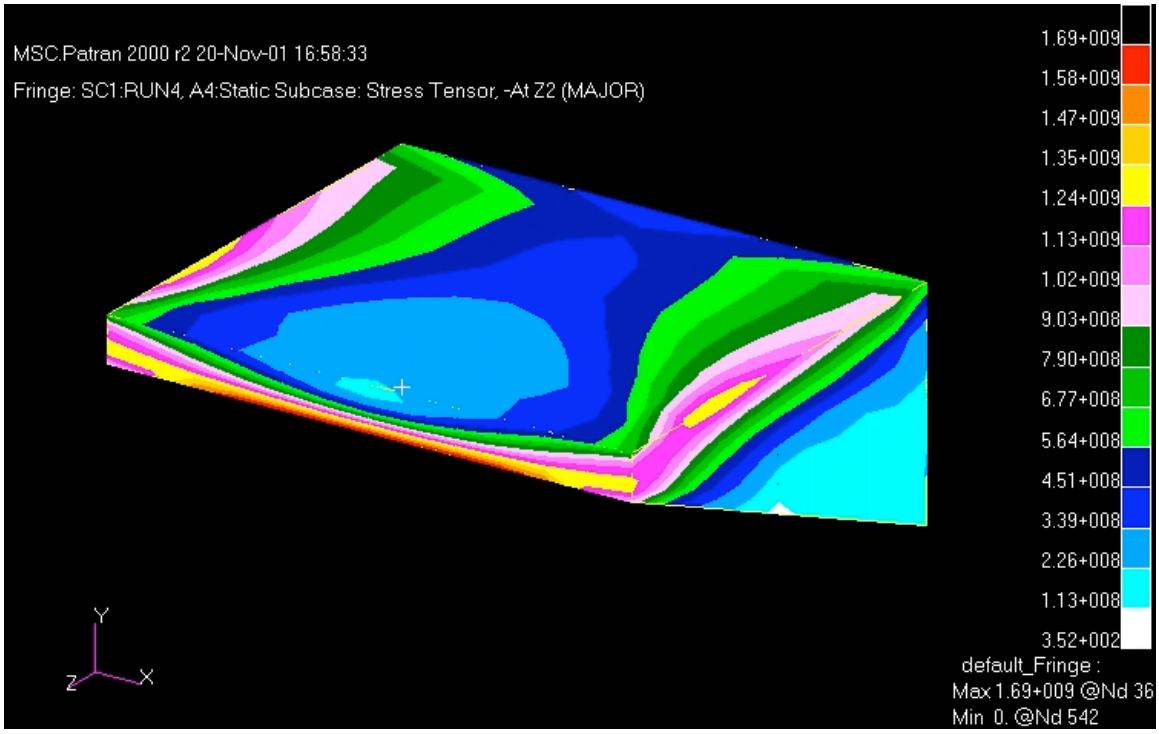

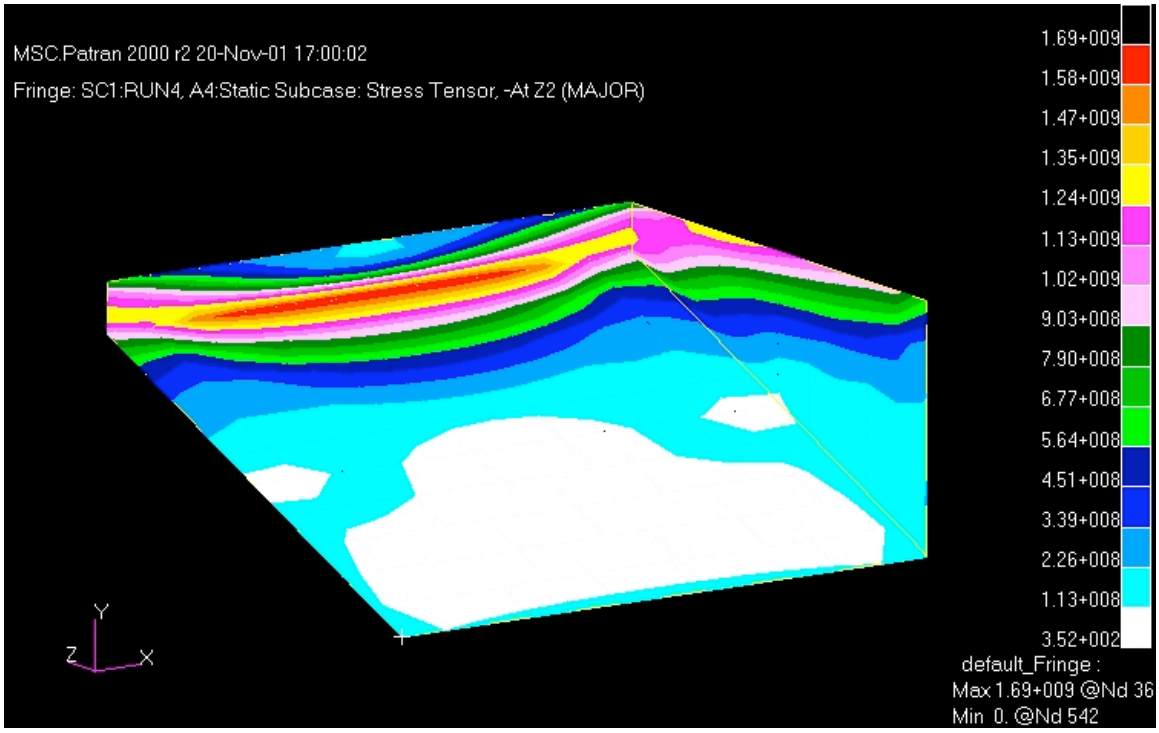

Figure 31: Stress Results for Run 4 (Stress in Pa)

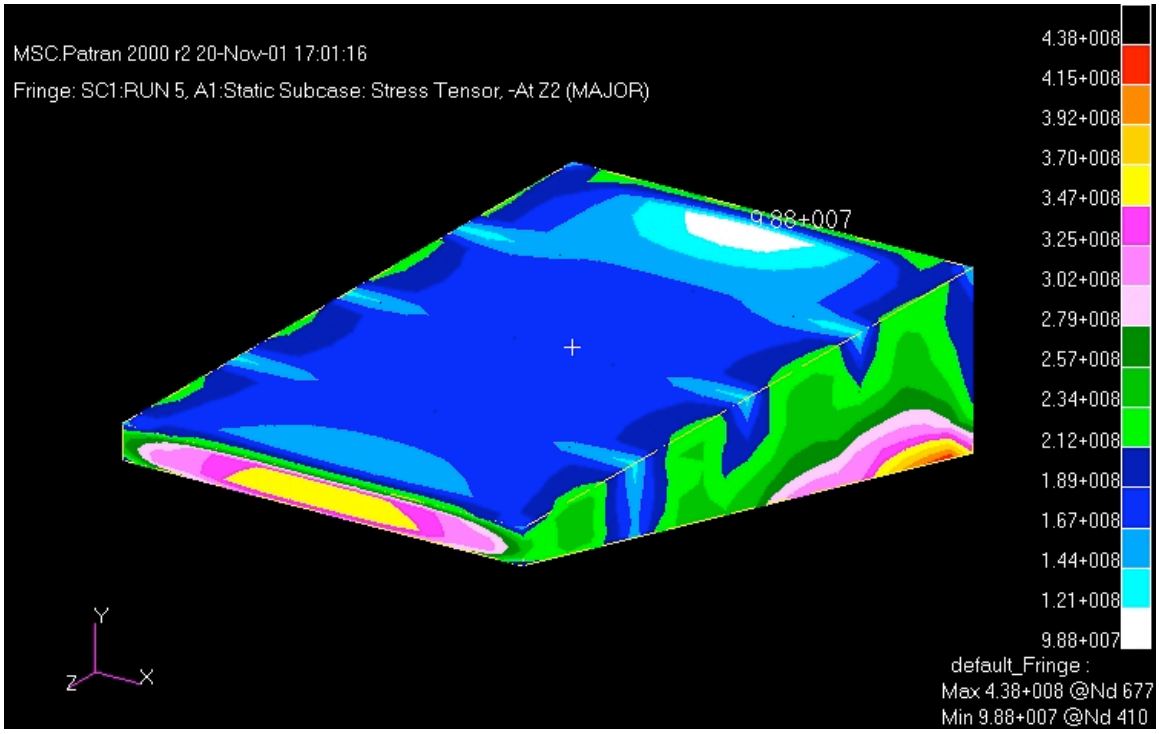

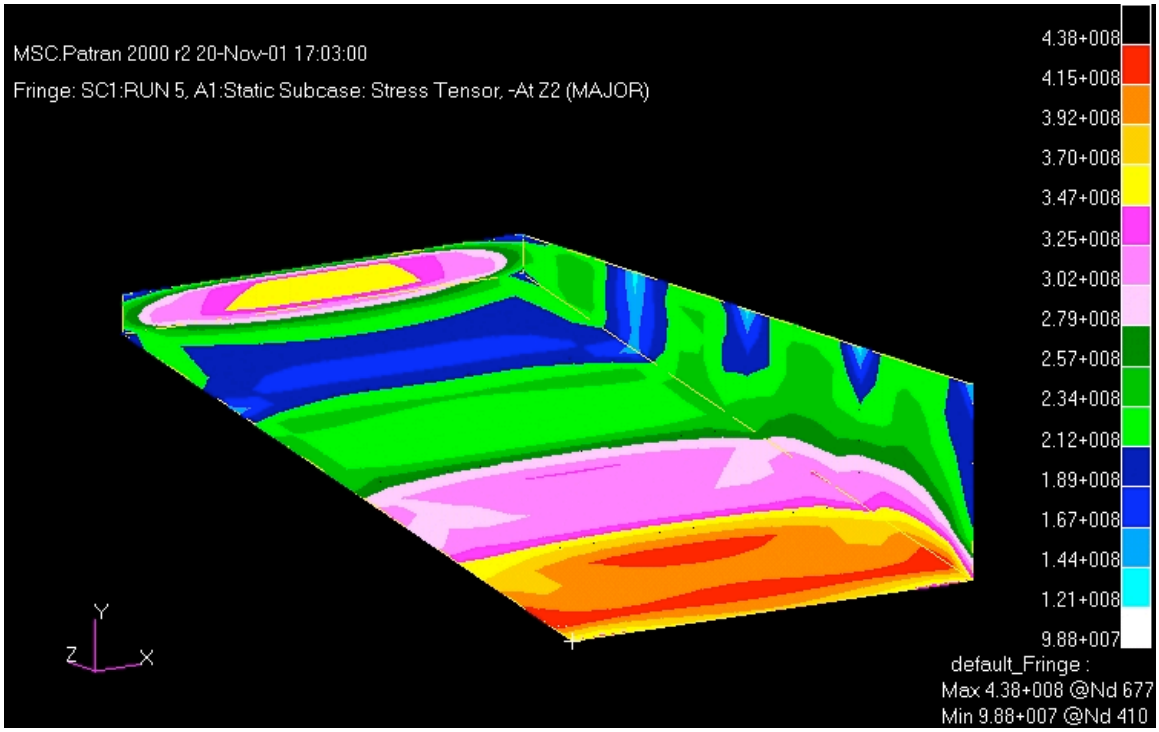

Figure 32: Stress Results for Run 5 (Stress in Pa)

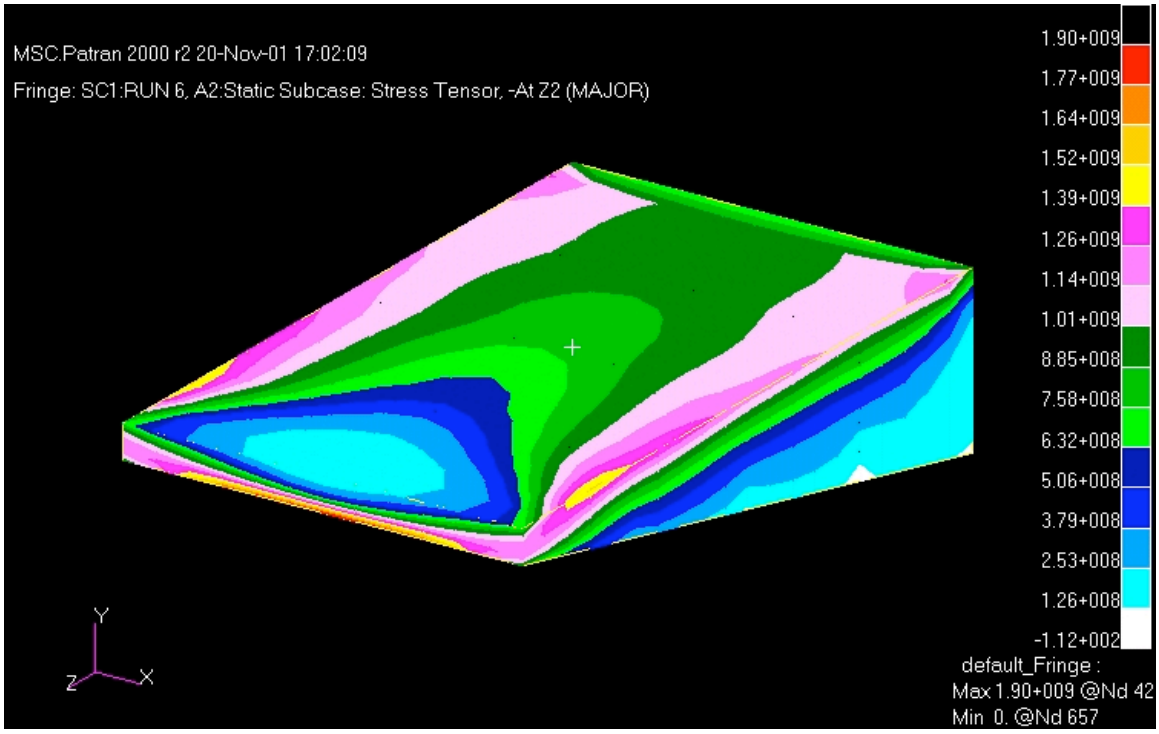

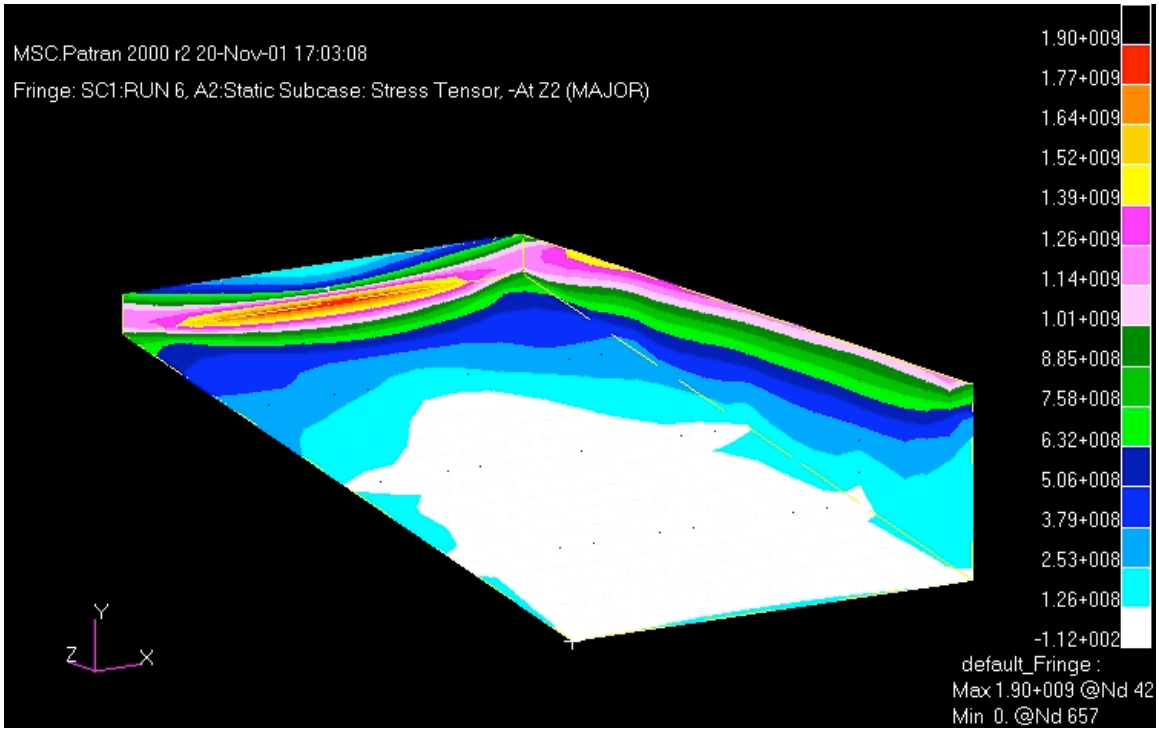

Figure 33: Stress Results for Run 6 (Stress in Pa)

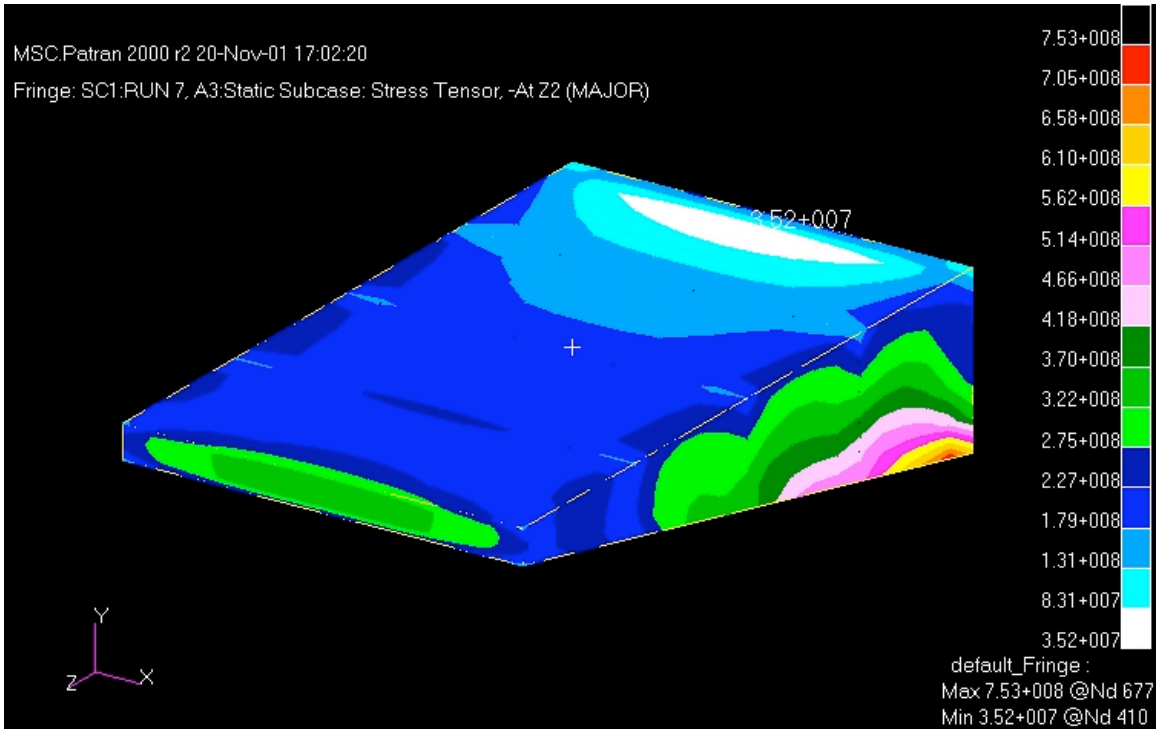

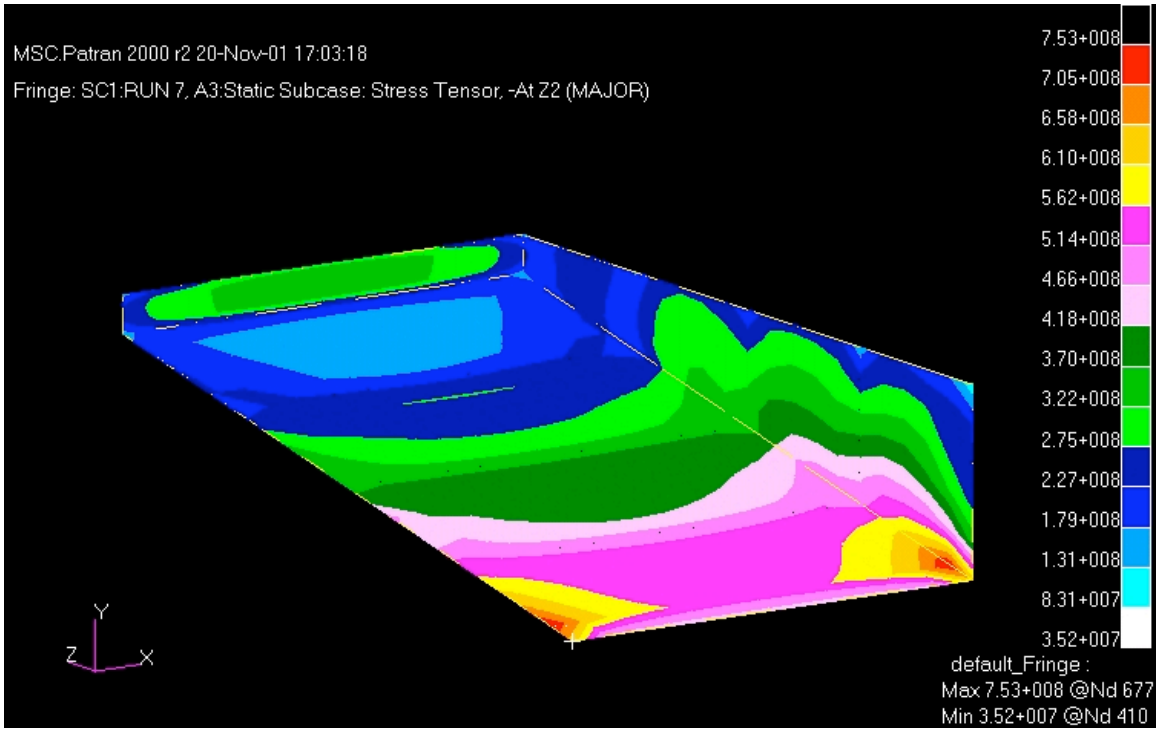

Figure 34: Stress Results for Run 7 (Stress in Pa)

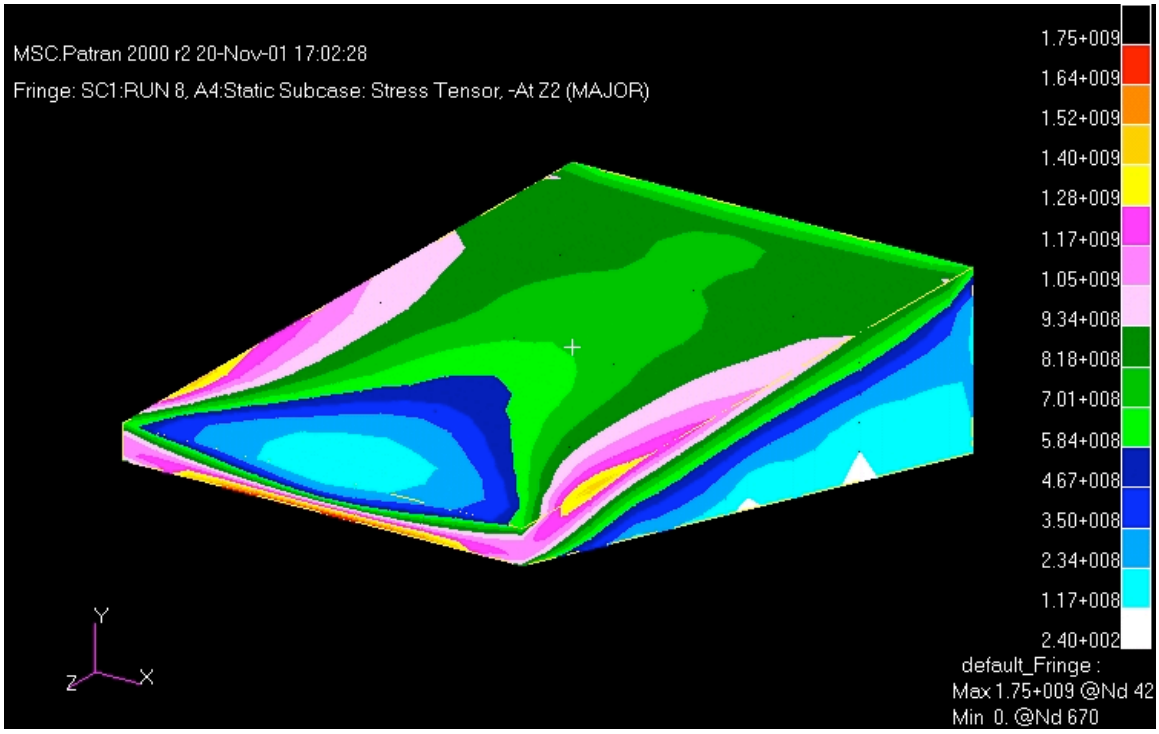

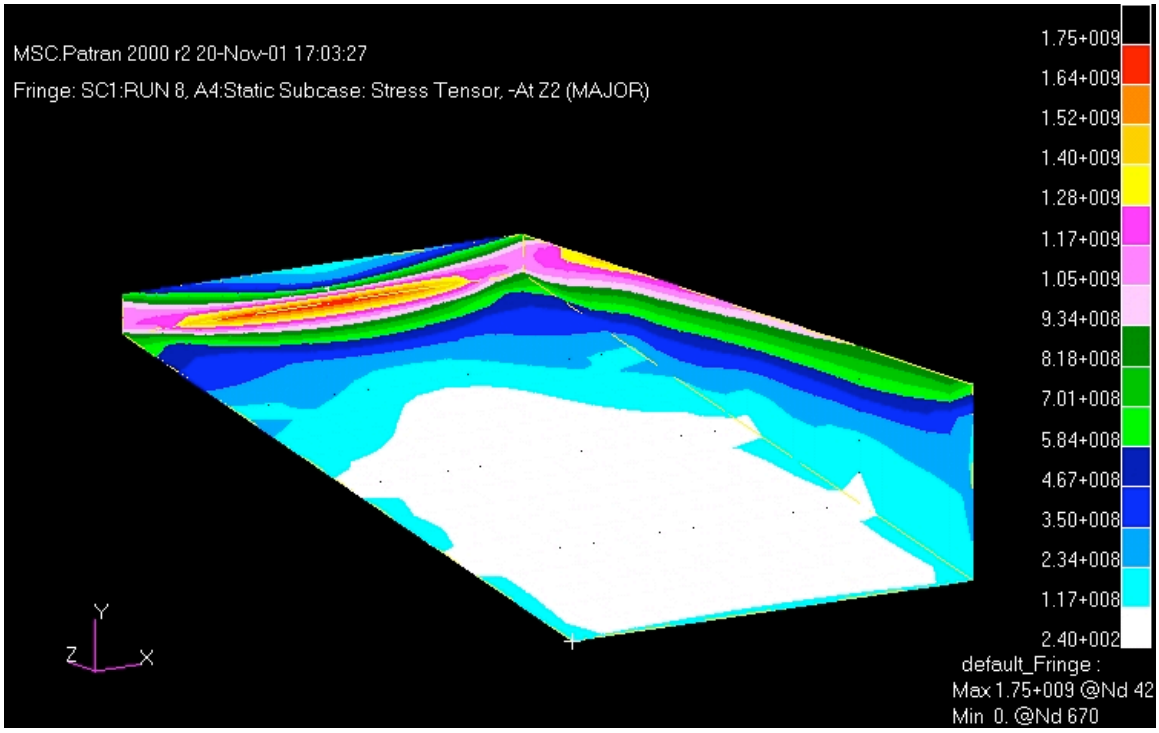

Figure 35: Stress Results for Run 8 (Stress in Pa)

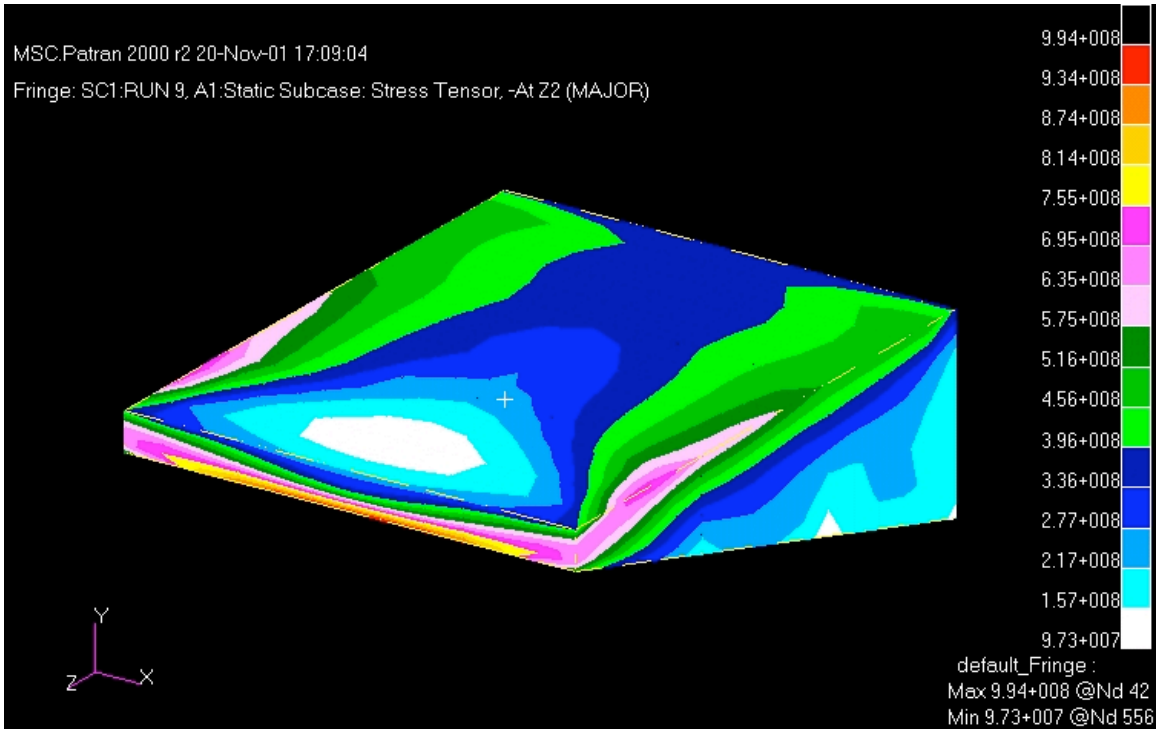

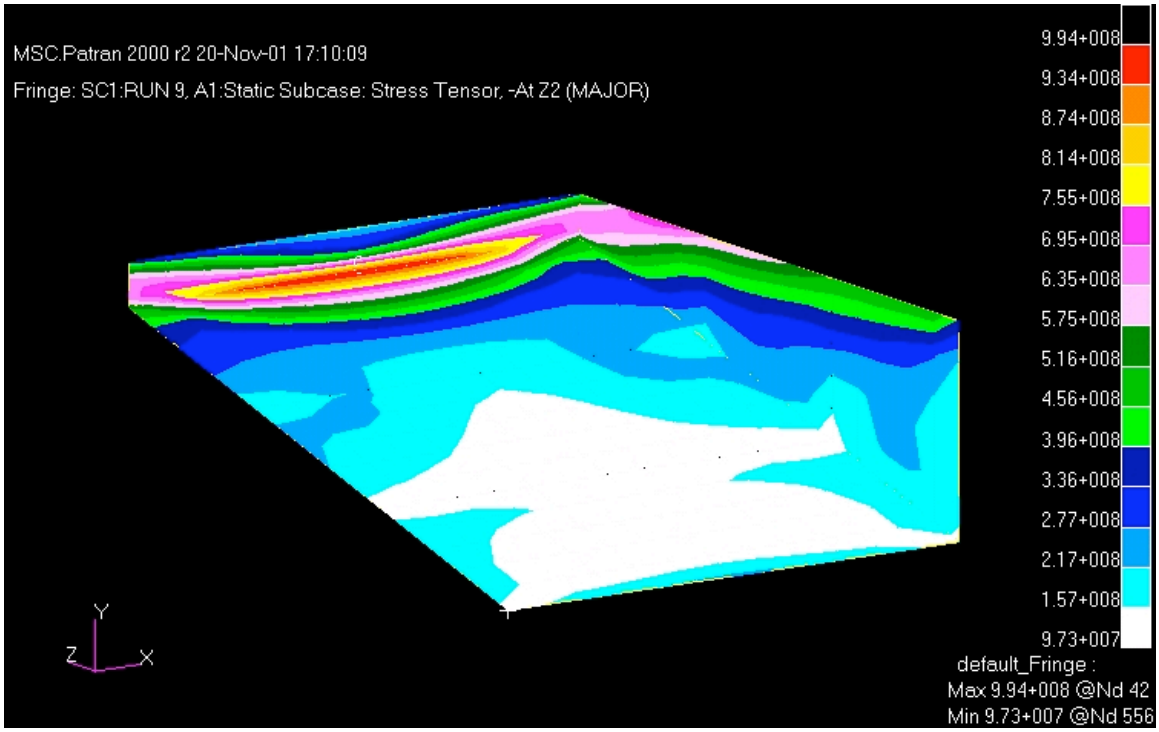

Figure 36: Stress Results for Run 9 (Stress in Pa)

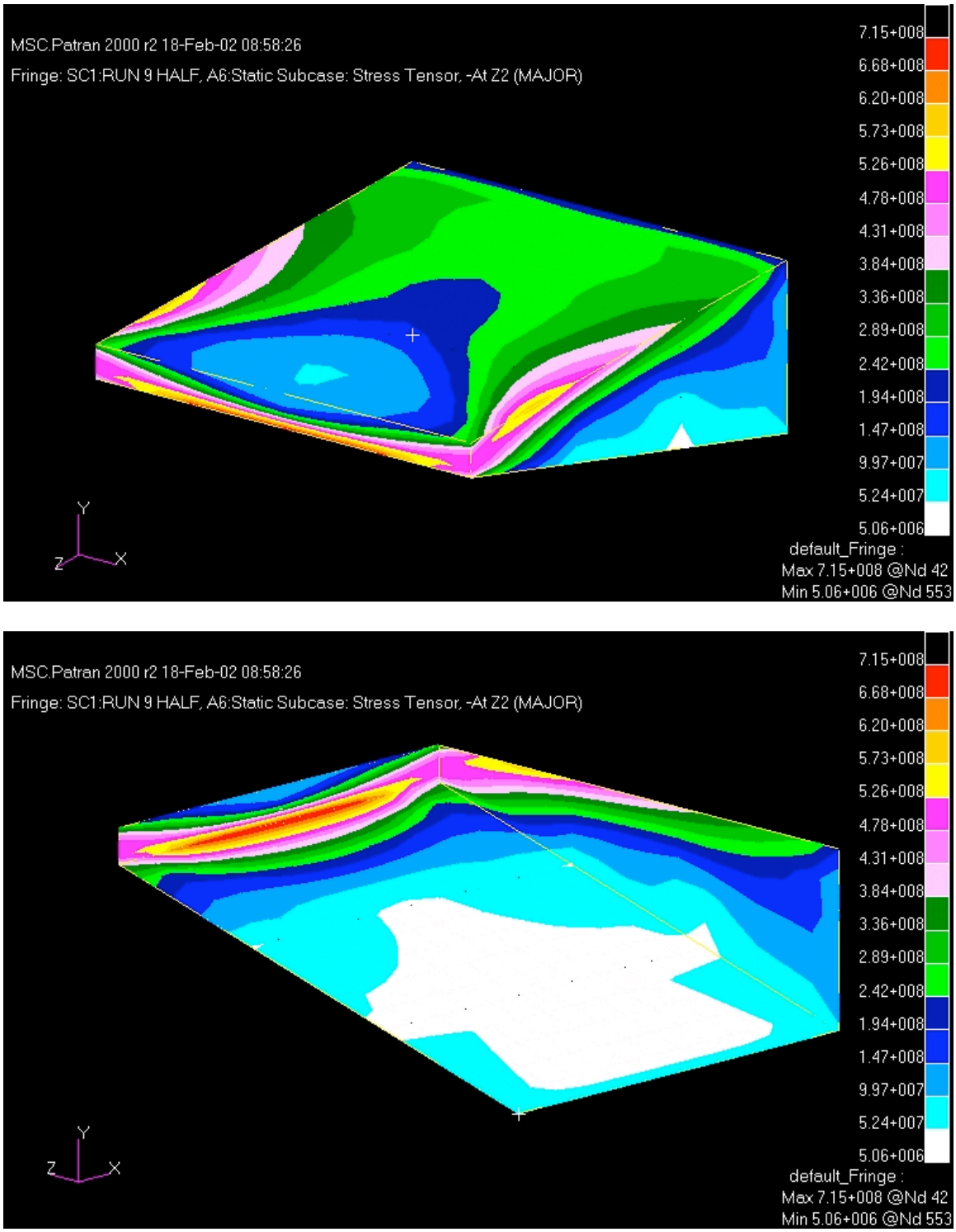

Figure 37: Stress Results for Run 9a (Stress in Pa)

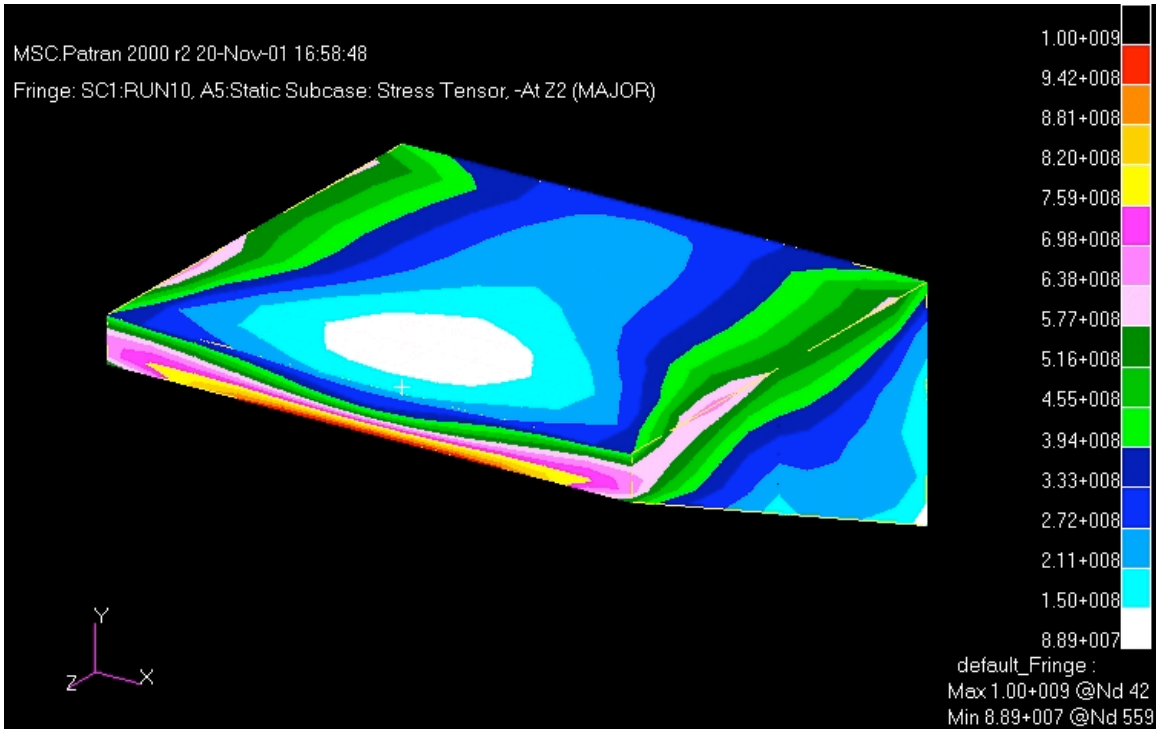

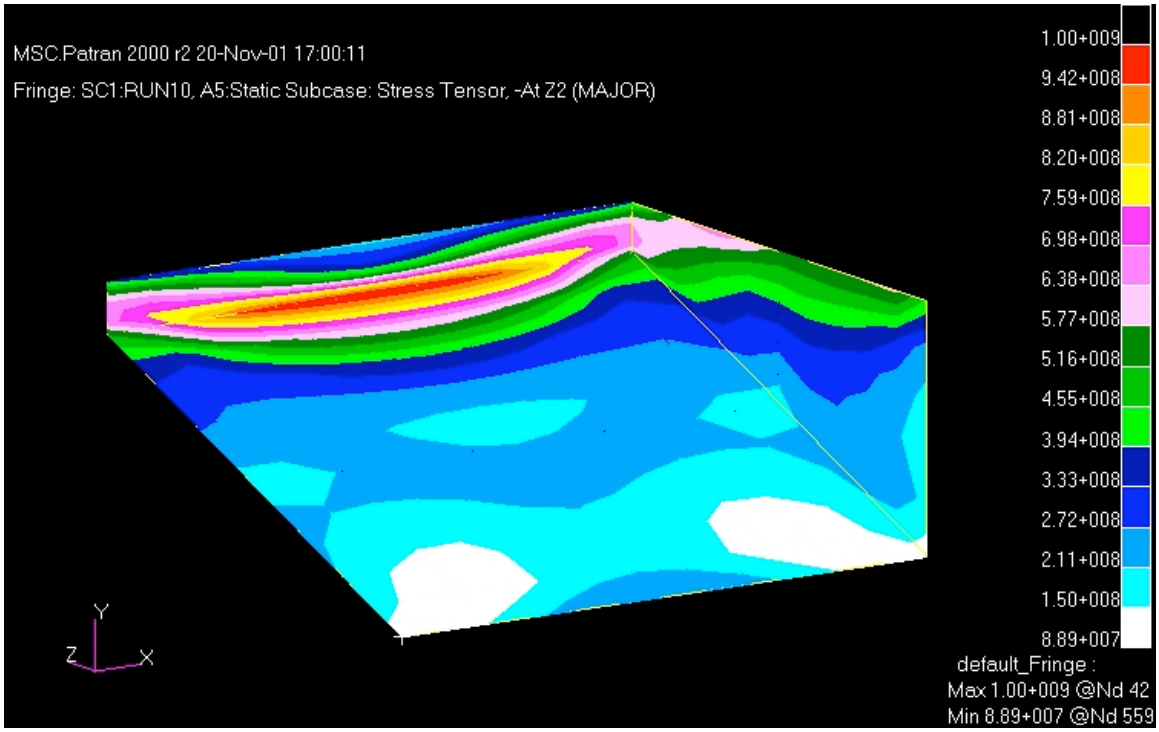

Figure 38: Stress Results for Run 10 (Stress in Pa)

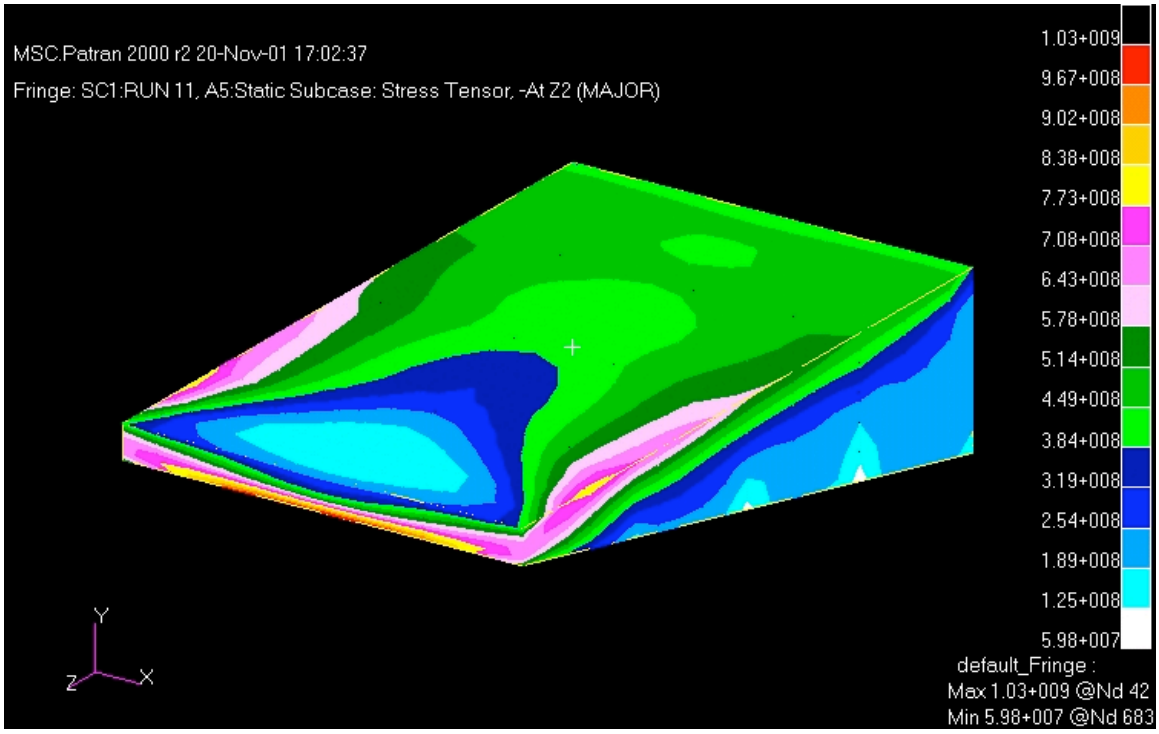

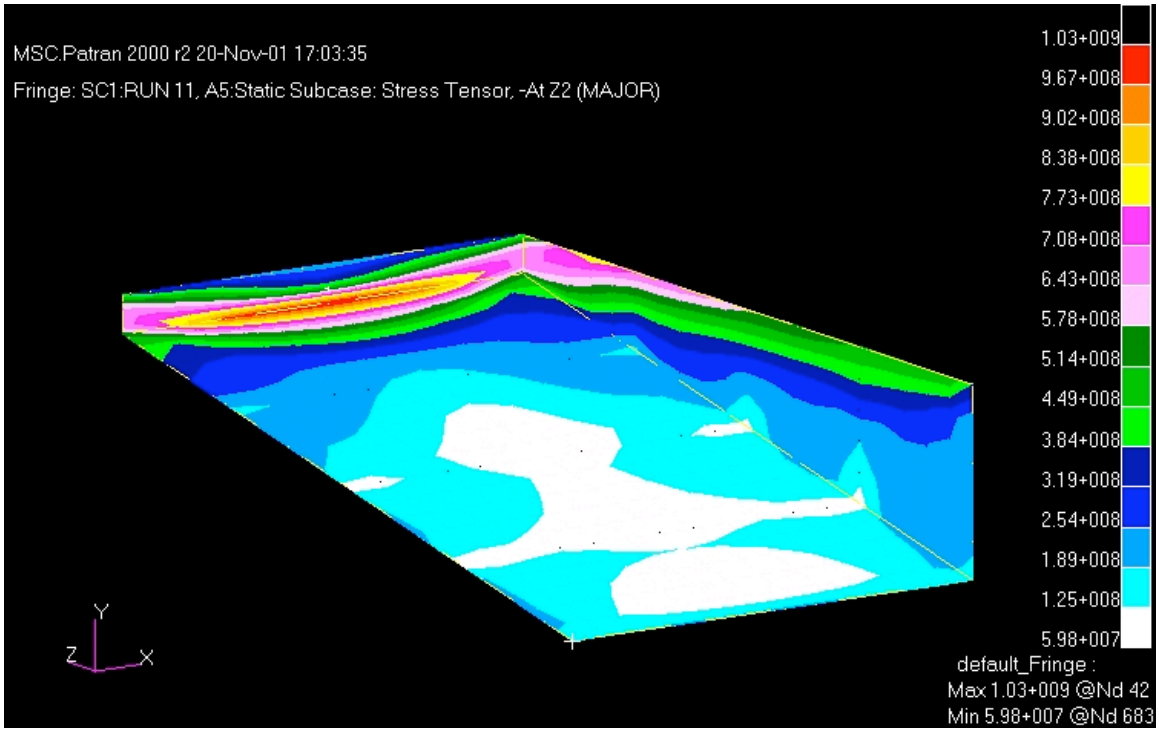

Figure 39: Stress Results for Run 11 (Stress in Pa)

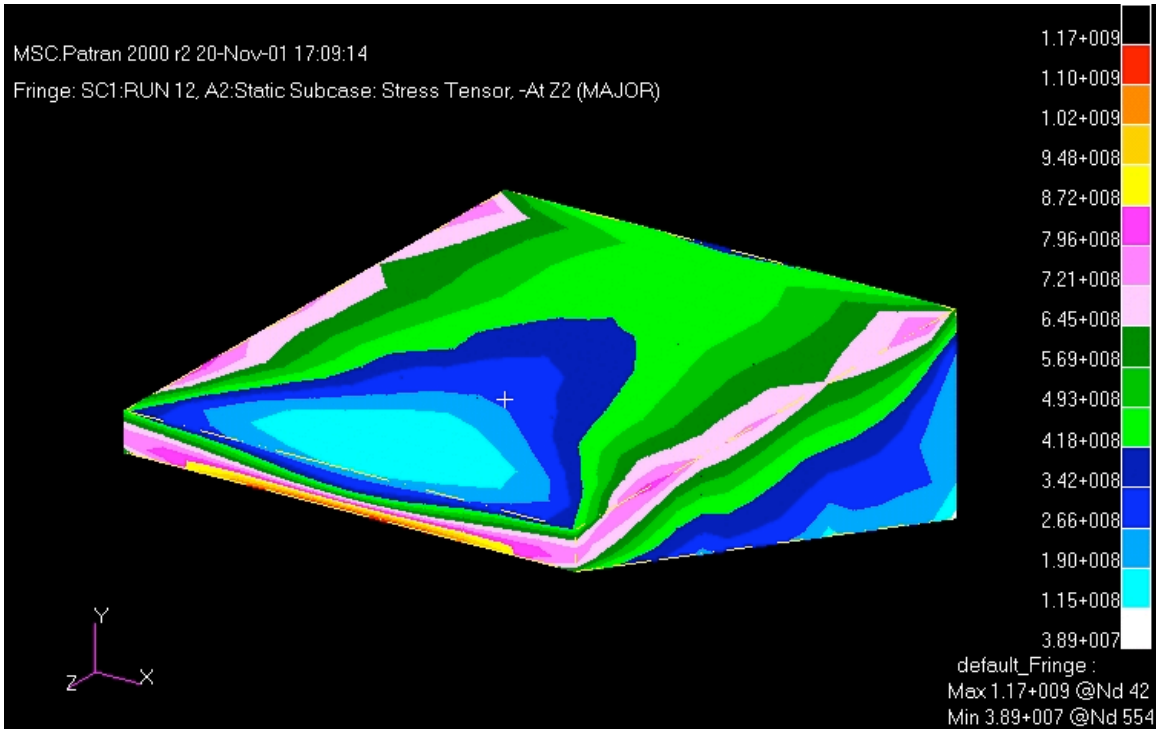

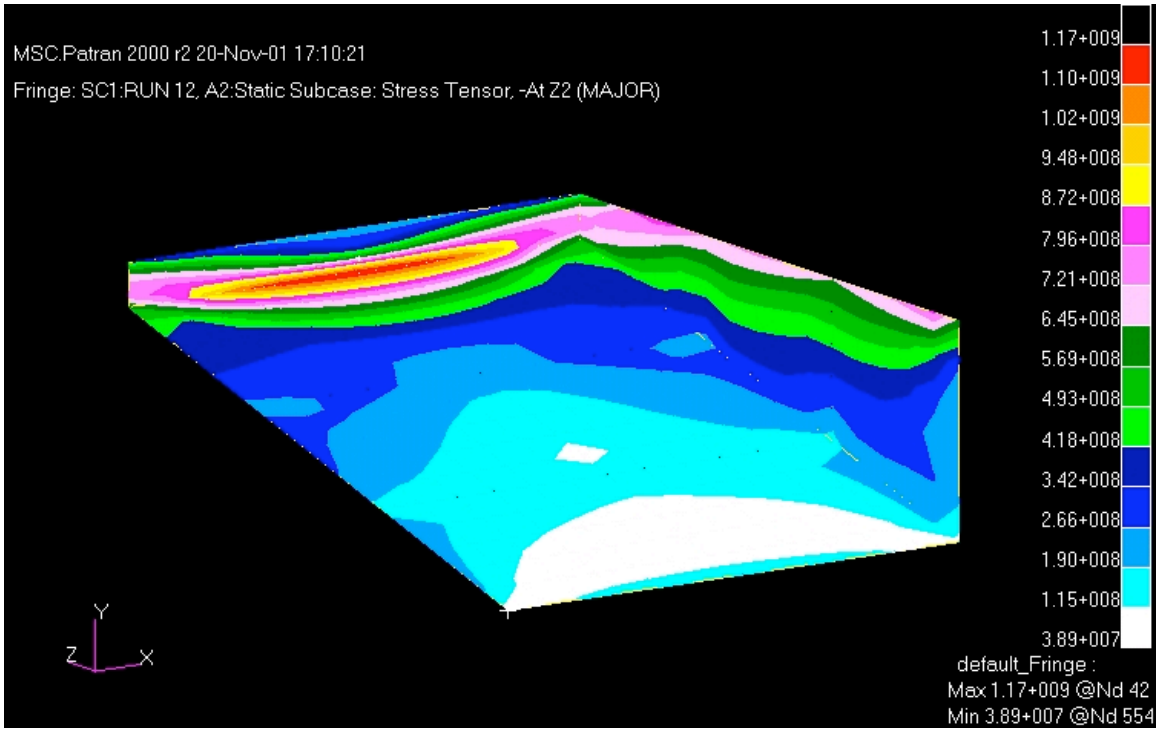

Figure 40: Stress Results for Run 12 (Stress in Pa)

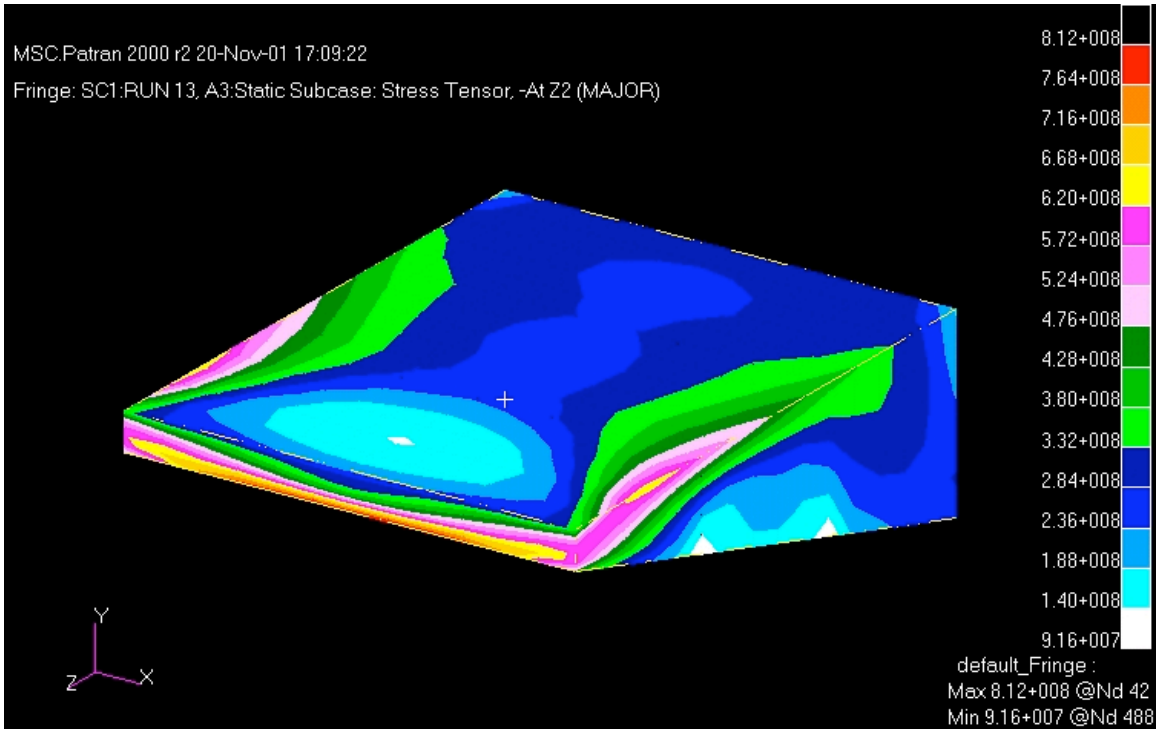

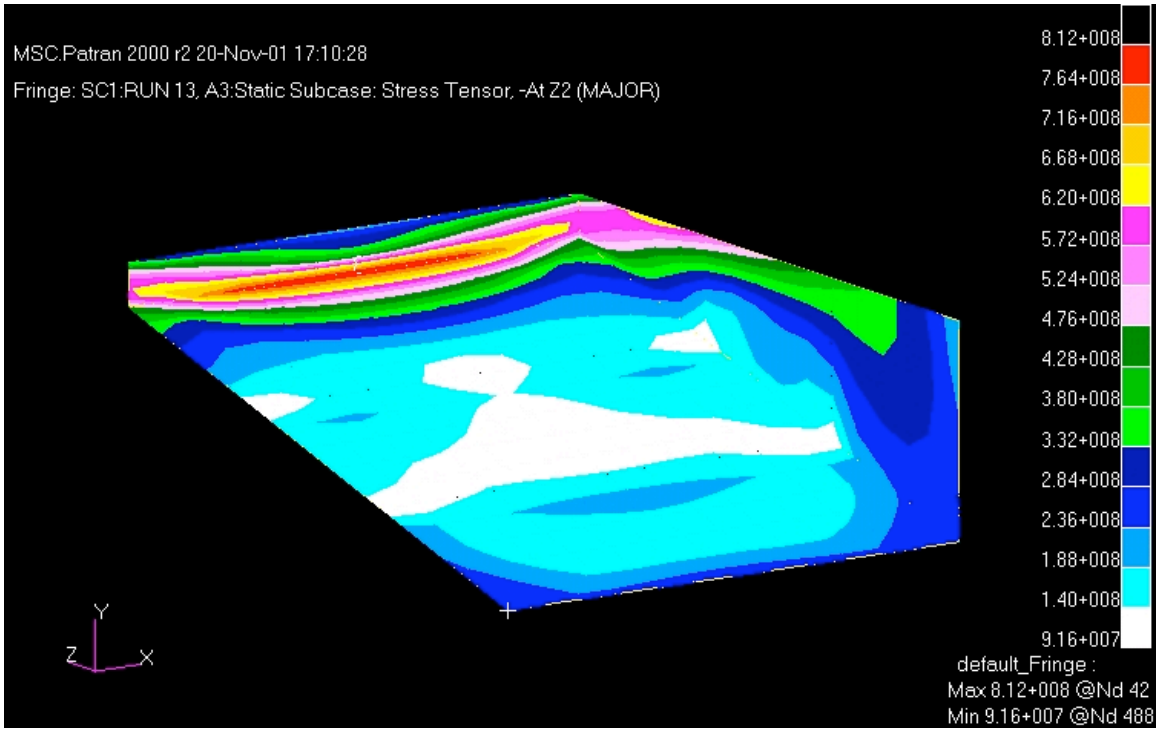

Figure 41: Stress Results for Run 13 (Stress in Pa)

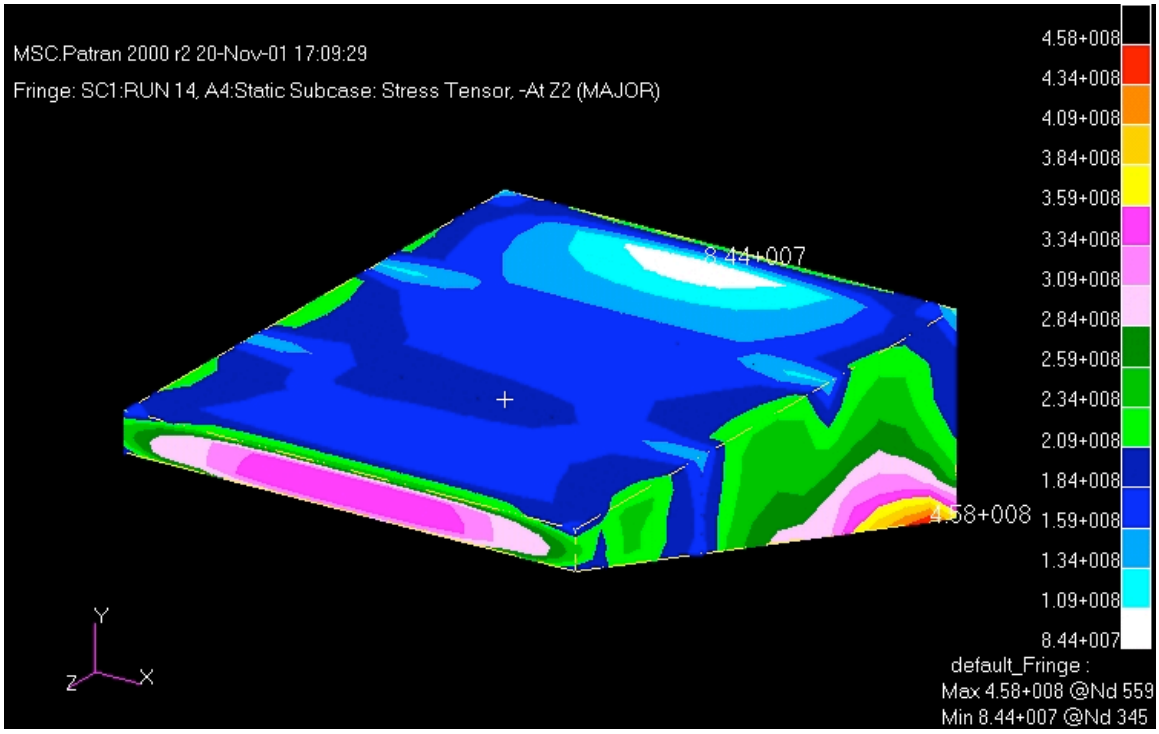

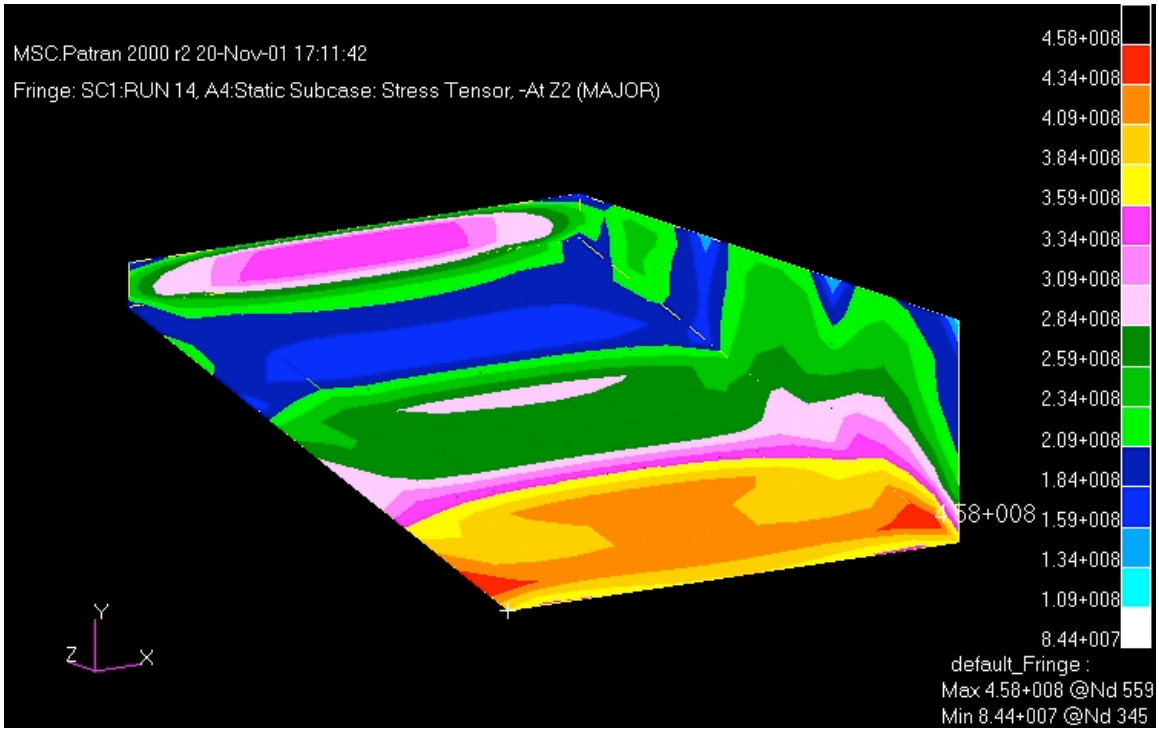

Figure 42: Stress Results for Run 14 (Stress in Pa)

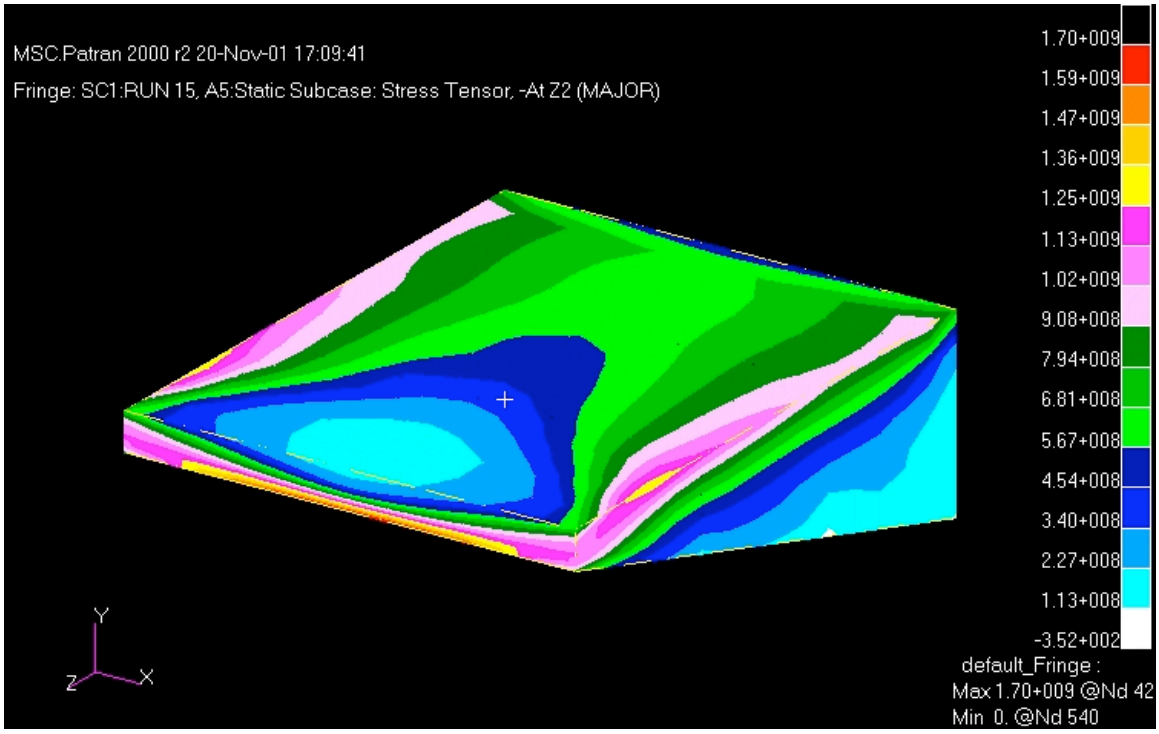

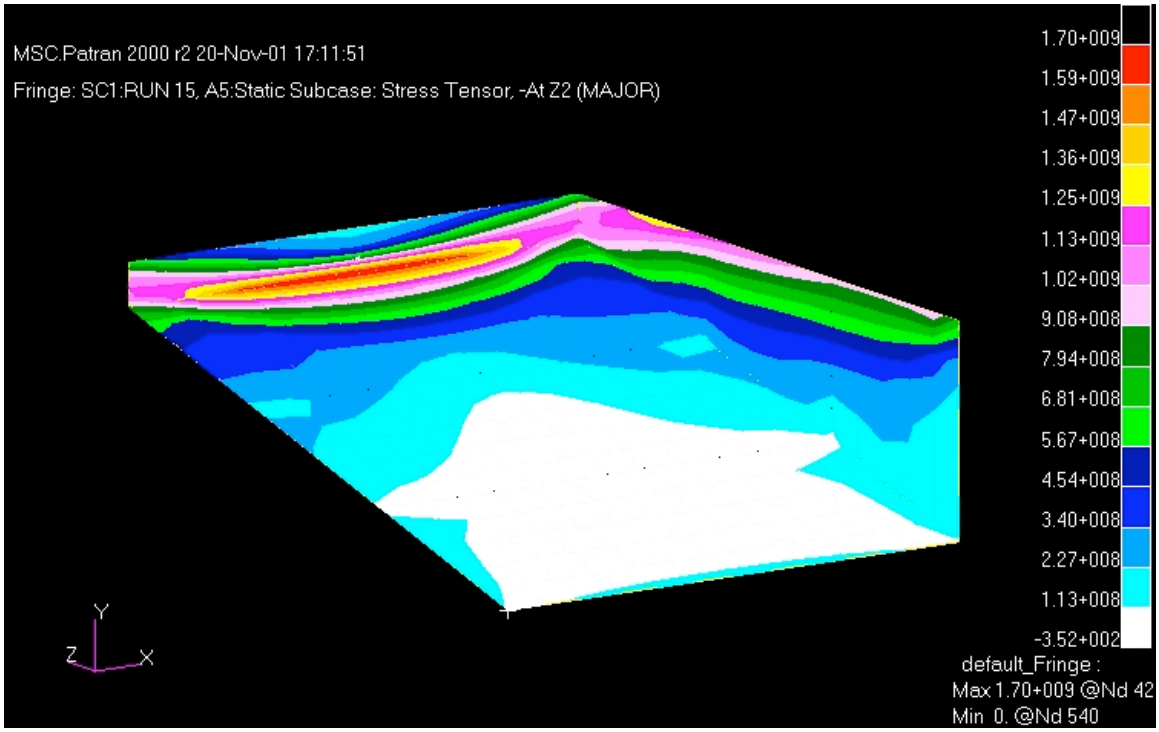

Figure 43: Stress Results for Run 15 (Stress in Pa)